$\mathcal{C}.\ 1$

GROUND-RUN TESTS WITH A BOGIE LANDING GEAR IN WATER AND SLUSH

by Robert C. Dreher and Walter B. Horne

Langley Research Center
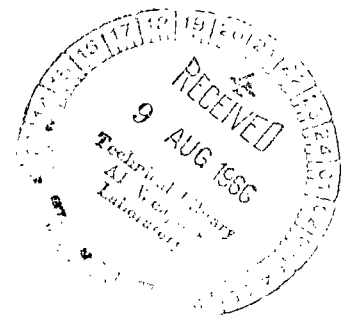*Langley Station, Hampton, Va.*

NASA TN D-3515

GROUND-RUN TESTS WITH A BOGIE LANDING GEAR

IN WATER AND SLUSH

By Robert C. Dreher and Walter B. Horne

Langley Research Center
Langley Station, Hampton, Va.

NATIONAL AERONAUTICS AND SPACE ADMINISTRATION

GROUND-RUN TESTS WITH A BOGIE LANDING GEAR

IN WATER AND SLUSH

By Robert C. Dreher and Walter B. Horne
Langley Research Center

SUMMARY

Ground-run tests were made with a bogie-type landing gear on water- and slush-covered runways to obtain data on fluid-displacement drag, wheel spin-down, wheel spray patterns, and fluid-spray drag. Tests were made with the normal four-wheel (dual tandem) configuration and with configurations consisting of one and two wheels at different locations on the bogie truck. The ground speeds ranged from 15 to 110 knots and the runway fluid depths ranged from 0.15 to 2.0 inches (0.38 to 5.08 centimeters). Tire inflation pressures were 25, 50, and 75 pounds per inch^2 (17.2, 34.5, and 51.7 newtons per centimeter^2), and the vertical load per tire was approximately 5000, 6000, or 12 000 pounds (22 200, 26 688, or 53 378 newtons) depending on the wheel configuration. Some tests were also made with a simulated wing flap mounted to the rear of the wheels in the take-off and landing positions. In addition, a few tests were made with a spray alleviator mounted between the wheels of the dual-tandem wheel configuration.

Results indicated that ground speed, vertical load, tire pressure, fluid density, fluid depth, and wheel location affected the fluid-displacement drag, the wheel spin-down characteristics, the wheel spray patterns, and the fluid-spray drag developed by this landing gear. Fluid spray impinging on the simulated wing flap in the landing position produced a maximum drag on the upper mass which was approximately 70 percent greater than that measured on the landing gear. The spray alleviator installed on the dual-tandem wheel configuration reduced the maximum fluid drag approximately 45 percent.

INTRODUCTION

The National Aeronautics and Space Administration for the past several years has been studying the adverse effects of water- and slush-covered runways on the take-off and landing performance of airplanes. In 1960, the NASA performed slush tests on a single airplane wheel at the Langley landing-loads track. On the basis of these tests, a method for predicting airplane take-off distance in slush was developed and is presented in reference 1. This method did not account for drag due to slush spray impinging on the airplane or for tire hydroplaning effects, since only the drag due to displacing the fluid on

the runway from the paths of the front wheels of the landing gear was considered. As a result of these tests and of full-scale tests of reference 2, the Federal Aviation Agency instituted the "1/2 inch rule" which prohibits jet-transport airplanes from taking off on runways covered with slush or water greater than 1/2 inch (1.27 centimeters) in depth.

However, uncertainties such as tire size, tire pressure, number of wheels, high forward speeds, and vertical load existed when the slush drag prediction method developed with the single wheel was applied to particular airplanes. Because of these uncertainties, it was believed that full-scale tests on a jet transport operating in slush would provide results which would be useful in confirming or refining the slush drag prediction method. Such tests were performed in the fall of 1961 by the FAA with NASA technical assistance on a commercial jet transport owned by the FAA. The results of these tests were reported in references 3, 4, and 5; some of these results are shown in figure 1. These results indicated that the effects on slush drag of slush-spray interference and impingement and of hydroplaning were large and, therefore, the simple theory of reference 1 was not adequate to predict slush drag.

In order to obtain information on runway fluid-displacement drag, wheel spin-down, wheel spray patterns, and fluid-spray drag, the NASA conducted ground-run tests on water- and slush-covered runways at the Langley landing-loads track. A four-wheel (dual tandem) bogie landing gear was used in these tests. Seven separate wheel configurations, six of which consisted of one and two wheels in different locations on the landing-gear truck and the normal four-wheel (dual tandem) configuration, were used during the tests. Tests were also made with a simulated wing flap mounted to the rear of the wheels and some tests were made with a fluid-spray-drag alleviator mounted on the bogie landing-gear truck. The tests were made at various ground speeds, tire pressures, runway fluid depths, and vertical loads.

The purpose of this paper is to present the results obtained during this investigation. These results show the effect of fluid-covered runways on landing-gear drag and wheel spin-down, the fluid spray patterns developed with the different wheel configurations, and the drag produced by fluid spray impinging on a simulated flap. In addition, the results show the possibility of reducing spray drag by means of an alleviator.

SYMBOLS

Measurements for this investigation were taken in U.S. Customary Units and equivalent values are indicated herein in the International System of Units (SI). Details concerning the use of SI together with physical constants and conversion factors are given in reference 6.

b_s	tire width, inches (centimeters)
b_{st}	tire width, inches (centimeters), at inflation pressure of 75 pounds per inch^2 (51.7 newtons per centimeter^2)
D_s	drag due to fluid, pounds (kilonewtons)
d_1	runway fluid depth, inches (centimeters)
d_{st}	reference runway fluid depth, 1.0 inch (2.54 centimeters)
$F_{z,g}$	vertical load on landing gear, pounds (newtons)
p	tire inflation pressure, pounds per inch^2 (newtons per centimeter^2)
V_G	ground speed, knots
V_P	tire hydroplaning speed, knots
$\dfrac{\omega_{wet}}{\omega_{dry}}$	ratio of wheel angular velocity on a wet runway to that on a dry runway surface

APPARATUS

Test Vehicle

This investigation was made at the Langley landing-loads track. The test vehicle of this facility is the carriage shown in figure 2 and weighs approximately 100 000 lb (444.8 kN). This carriage is catapulted by a hydraulic jet to speeds up to 120 knots along steel rails which are 30 ft (9.14 m) apart and 2200 ft (670.56 m) long. The carriage straddles a concrete runway which has a surface similar to airport runways. A vertical drop carriage to which the test landing gear is attached is incorporated within the main carriage. Further information on the operation of this facility is given in reference 7.

Landing Gear

The dual-tandem bogie landing gear used in this investigation was equipped with 12.50-16, 38-inch-nominal-diameter (96.52 cm), type III, 10-ply-rating, dimple-tread tires. A schematic drawing of the test fixture and landing gear is shown in figure 3. The oleo-pneumatic shock strut of the gear was replaced by an 8-inch-diameter (20.32 cm)

bar. Due to the geometry of the landing gear, 46 percent of the total static vertical load was carried on the front axle and 54 percent on the rear axle.

Wheel Configurations

Seven configurations of the landing-gear wheels were used during the tests. These configurations, in order of testing, are shown by the sketches in table I. For configurations I, IV, V, and IA the landing gear was free to pitch about the truck-beam pivot since the pitch snubbers were removed. A wire rope fastened between the front axle and the test fixture prevented the gear from pitching down to an excessive degree when it was airborne. Configuration I was the normal condition in which all four wheels were mounted on the landing gear. In configuration II the two rear wheels were removed and replaced by steel bars which were attached from the wheel axles to the upper part of the vertical drop carriage. Similarly, in configuration III the two front wheels were removed and replaced by steel bars. A diagonal wheel arrangement was obtained in configuration IV by removing the right front and left rear wheels. Configuration V consisted of two single wheels in tandem. Single wheel configurations VI and VII consisted of the left front and the rear wheel, respectively. A spray-drag alleviator was attached between the dual tandem wheels for some of the tests; this configuration was designated configuration IA.

Water and Slush Trough

Concrete dikes placed along the sides of the track runway formed a trough 9 ft (2.74 m) wide and 512 ft (156.06 m) long as shown in figure 4. Temporary dams of a puttylike material were placed at each end of the trough to retain the slush and water for testing.

Slush was made by the ice-crushing machine shown in figure 5. Photographs and a description of a similar slush-laying operation are given in reference 5. The crushed ice was first leveled manually to the approximate test depth desired. Just before the start of a test run, the slush was trimmed to the desired test depth by the machine shown in figure 6. The crushed ice was allowed to melt to a slushy condition before a test. The average specific gravity of the slush used in this investigation was 0.88.

TEST PROCEDURE

The runway fluid depth d_1 and the slush density, in the case of slush tests, were measured immediately prior to each test at the eight stations along the trough shown in figure 4. Before each test, the vertical drop carriage was positioned so that the landing-gear wheels were approximately 2.0 in. (5.08 cm) above the runway surface. Then the test carriage was catapulted to the desired ground speed by means of the hydraulic jet. In order to minimize landing-gear oscillations during the tests, the landing gear was

4

allowed to contact the runway well ahead of the test section. Views of the slush bed before and after a typical test are shown in figures 7 and 8, respectively. All tests were made with freely rolling (unbraked) wheels.

In the investigation, a series of tests was made with each of the wheel configurations shown in table I. The ground speed V_G ranged from 15 to 110 knots. Tire inflation pressures p of 25, 50, and 75 lb/in^2 (17.2, 34.5, and 51.7 N/cm^2) were used and the runway fluid depth d_1 ranged from 0.15 to 2.0 in. (0.38 to 5.08 cm) for the water tests and from approximately 1.0 to 2.0 in. (2.54 to 5.08 cm) for the slush tests. The vertical load per tire for the different wheel configurations is given in table I. In addition, a few tests were made on the dual tandem wheels (configuration I) with a vertical load of approximately 12 000 lb (53 378 N). A simulated wing flap was mounted to the rear of the landing-gear wheels as shown in figure 9. This flap was mounted at an angle of 22° during tests with all the wheel configurations and also at an angle of 55° with configuration VI. Tests were also made with a spray-drag alleviator mounted on the dual tandem wheels (configuration IA) as shown in figure 10.

INSTRUMENTATION

The drag load cell shown on the sketch in figure 3 was used to measure the drag forces developed between the landing-gear wheels and the runway whereas the upper mass drag dynamometer measured the total drag developed on the landing gear and the simulated wing flap (fig. 9). The difference between these two drag measurements gives the drag load experienced by the simulated wing flap alone. Instrumentation was provided to measure the angular velocity and displacement of each landing-gear wheel and the vertical displacement of the vertical drop carriage. The horizontal displacement and ground speed of the main carriage were obtained by means of a photocell. The light source from the photocell was interrupted at 10-ft (3.048 m) intervals along the runway and produced a pulse on an oscillograph-record trace. The electrical outputs of the instrumentation were continuously recorded during the tests by means of an 18-channel oscillograph.

Several 16-mm motion-picture cameras operating at 200 frames per second and one 70-mm camera operating at 10 frames per second were mounted at various locations on the main carriage in order to obtain motion pictures of the landing-gear wheels during each test.

RESULTS AND DISCUSSION

Previous research conducted on fluid-covered runways clearly shows that the phenomenon of tire hydroplaning can greatly influence the tire-ground forces developed

on aircraft. Available experimental data on hydroplaning were summarized in refer-
ence 8, in which the following simple expression was developed for estimating tire hydro-
planing speed

$$V_P = 9\sqrt{p} \tag{1}$$

where

V_P tire hydroplaning speed, knots

p tire inflation pressure, lb/in^2 (N/cm^2)

Since one of the main purposes of this investigation was to determine fluid drag
effects on a landing gear under hydroplaning conditions, this equation was used to select
tire pressures for study that would cause the test tires to hydroplane well before the
maximum speed capability (approximately 120 knots) of the test carriage was reached.

Fluid Drag Parameter

When an unbraked tire rolls on a fluid-covered runway, as in airplane take-off, the
moving tire contacts and displaces the stationary runway fluid. The resulting change in
momentum of the fluid creates hydrodynamic pressures that react on the tire and runway
surfaces. The horizontal component of the resulting hydrodynamic pressure force is
termed "fluid-displacement drag" and the vertical component, "fluid-displacement lift."
Additional fluid forces termed "fluid-spray thrust or drag" and "fluid-spray lift" are
created on aircraft when some of this displaced runway fluid in the form of spray sub-
sequently impinges on other parts of the aircraft such as the tires, landing gear, and
flaps.

The fluid drag parameter is defined as the incremental drag developed from all
fluid-displacement and fluid-spray drag sources normalized to an effective water depth
of 1.0 inch (2.54 cm). Values of this parameter were obtained by subtracting the dry-
runway rolling resistance of the tires from total drag values measured by the test instru-
mentation. This incremental drag was then normalized to an effective fluid depth of
1.0 inch by multiplying by the ratio of a reference or standard fluid depth (1.0 inch) to
the test fluid depth. For the slush runs, this result was divided by the specific gravity
of the slush to normalize the drag data to an effective water density. This normalizing
procedure was necessary because it was practically impossible to duplicate fluid depths
from run to run because of different slush melting rates experienced at different times of
day and from day to day. It was also found that water depths could vary considerably
during some runs because of wind effects. Results of this investigation indicated that the

fluid drag parameter is affected by various factors. The effect of several of these factors is discussed in the following sections.

Effect of ground speed.- The variation of the fluid drag parameter with ground speed for the dual tandem wheels (configuration I) with tire inflation pressures of 25, 50, and 75 lb/in^2 (17.2, 34.5, and 51.7 N/cm^2) on water- and slush-covered runways is shown in figure 11. The fluid depths ranged from 0.5 to 2.0 in. (1.27 to 5.08 cm). The curves faired through the data indicate that the drag parameter increases parabolically with increasing ground speed until a speed near the predicted hydroplaning speed V_p is reached. After this speed is attained, the drag decreases. This decrease is attributed to the tires riding up in the fluid and thus displacing less fluid from the runway and to the change in spray patterns.

Effect of fluid density.- Figure 11 also shows that there is very little difference in the values of the drag parameter obtained during tests through water (circles) or slush (squares). Therefore, normalizing the slush data to a standard of 1.0 in. (2.54 cm) of water tends to confirm the results shown in reference 9 that fluid drag is proportional to fluid density.

Effect of tire width.- At ground speeds before peak drag, the slope of the drag parameter curves increases as the tire pressure is decreased, as shown in figure 12(a). With the same vertical load, the tire width b_s increases from 10.1 in. (25.65 cm) at 75 lb/in^2 (51.7 N/cm^2) to 12.0 in. (30.48 cm) at 25 lb/in^2 (17.2 N/cm^2). The consequently greater tire frontal area exposed to the runway fluid for the lower tire pressure causes more fluid to be displaced from the path of the wheel and thereby causes an increase in the drag parameter. When the values of the drag parameters obtained with tire pressures of 25 and 50 lb/in^2 (17.2 and 34.5 N/cm^2) are normalized in terms of b_{st}, the tire width at 75 lb/in^2, the curves shown in figure 12(b) are obtained. It can be seen from this figure that this normalizing procedure causes the three curves to be practically the same at ground speeds less than the hydroplaning speed. This result tends to validate the assumption made in reference 1 that fluid drag is proportional to the width of the tire at the intersection of it and the fluid surfaces on the runway.

Effect of tire pressure.- Figure 12(a) also shows the large effect on the drag parameter created by changes in tire inflation pressure. For example, decreasing the tire pressure from 75 to 25 lb/in^2 (51.7 to 17.2 N/cm^2) reduces the maximum drag on the landing gear by 50 percent and changes the location of the drag peak from approximately 78 to 45 knots. This effect is, of course, the result of tire hydroplaning and leads to the conclusion that reducing the tire inflation pressure will in turn reduce the maximum fluid drag experienced by a landing gear. It should be pointed out that this reduction in tire inflation pressure will also decrease the ground speed at which the tire loses contact with the ground (tire loses its ability to develop braking and cornering traction) as

evidenced by the shift of the drag peak from 78 to 45 knots occurring when the tire pressure is reduced from 75 to 25 lb/in^2.

Effect of wheel configuration.- Another factor which affects values of the drag parameter is the location of the wheels on the bogie landing gear. Figure 13(a) summarizes the variation of drag parameter with ground speed in water and slush for the different wheel configurations at a tire pressure of 75 lb/in^2 (51.7 N/cm^2). This figure shows that the rear-mounted dual and single wheels (configurations III and VII) experience less drag than the corresponding front-mounted wheels (configurations II and VI). It is believed that these differences in drag are due to fluid spray. Spray from the front-mounted wheels is thrown rearward and impinges on various members of the landing-gear structure which are to the rear of the wheels and thereby increases the drag. The spray from the rear-mounted wheels does not increase the drag on the landing gear since none of the structure is to the rear of these wheels. In addition, motion pictures taken during the tests show that spray from the bow wave of the rear-mounted wheels impinges on the landing-gear structure ahead of the wheels and produces thrust which decreases the drag parameter.

The effect of wheel configuration on the drag parameter is also shown in this figure by the curves representing the diagonal wheels and the single tandem wheels (configurations IV and V). Even though these two configurations were similar, the maximum drag developed by the diagonal wheel configuration was more than twice that developed by the single-tandem wheel configuration. This result is also shown in figure 13(b) which gives the variation of drag parameter with ground speed for configurations I, III, IV, and V at a tire pressure of 25 lb/in^2 (17.2 N/cm^2) and was due to fluid-displacement drag as well as fluid-spray drag. In the diagonal wheel configuration, both the front and the rear wheels were, in effect, leading wheels in that each had to displace runway fluid, whereas in the single-tandem wheel configuration the front wheel displaced most, if not all, of the fluid from the path of the rear wheel. The diagonal wheel configuration experienced more fluid-spray drag since spray thrown to the side and rearward by the front wheel impinged directly on the rear wheel.

The values of fluid drag factor given in table I also show the effect of wheel location on the drag parameter. This factor was obtained by dividing the maximum value of the drag parameter obtained with each wheel configuration by the maximum value of the drag parameter obtained with the single-rear wheel configuration corrected for vertical load. In reference 10, the prediction was made that landing-gear-wheel location might influence fluid drag considerably. For example, this reference indicated that dual wheels (side by side) should experience more than twice the drag of a single wheel and single tandem wheels should experience considerably less. The values of fluid drag factor shown in table I tend generally to confirm this prediction.

Effect of vertical load.- The effect of vertical load on the drag parameter can be seen in figure 13(a). The curves representing the values of the drag parameter for the two single wheel configurations (VI and VII) are near those obtained with the single tandem wheels (configuration V) and are apparently due to load per tire. As shown in the figure, the total vertical load was 12 000 lb (53 378 N) for all three configurations. Hence, the load per tire for the single wheel configurations was approximately twice that for the single-tandem wheel configuration; this greater load produced a greater tire deflection and, consequently, a larger tire footprint width. Therefore, the wheels of these two single wheel configurations displaced more fluid from the runway, which resulted in greater values of drag parameter.

Wheel Spin-Down

An easily observed indication of tire hydroplaning is wheel spin-down. On a dry surface the spin-up moment produced on the tire by surface friction and tire deformation is balanced by a spin-down moment which is created by a forward shift of the vertical ground reaction. When the tire rolls on a fluid-covered runway, a wedge of fluid detaches the tire footprint from the runway surface and makes the spin-up moment tend toward a zero value. This wedge of fluid also causes the center of pressure of the vertical ground reaction on the tire to move farther forward of the axle and thereby creates a larger spin-down moment. At some critical speed, usually near the hydroplaning speed, this spin-down moment exceeds the total spin-up moment from all the drag sources so that the tire slows down and under certain conditions comes to a complete stop. Motion pictures of this phenomenon are shown in reference 11.

In order to determine the wheel spin-down characteristics on fluid-covered runways, the ratio of the measured wheel angular velocity on a wet runway surface to that on a dry runway surface $\frac{\omega_{wet}}{\omega_{dry}}$ was computed for each wheel configuration and plotted against the distance the landing gear traveled through the runway fluid at several ground speeds. These data and related data for the different wheel configurations are presented in figures 14 to 21. The ground speed at which the wheels enter and leave the fluid trough is given by the speed range shown in the figures. Several factors which influence wheel spin-down characteristics are discussed in the following sections.

Effect of ground speed.- Data obtained during this investigation indicate that wheel spin-down did not occur on leading wheels of the landing-gear configurations investigated until the ground speed either approached or exceeded the hydroplaning speed (determined from eq. (1)). Figure 14 shows this effect for the single tandem wheels (configuration V) and the dual wheels (configuration III) at a tire inflation pressure of 25 lb/in^2 (17.2 N/cm^2) in approximately 1.0 in. (2.54 cm) of water. The wheels did not spin down

until the ground speed was near the predicted hydroplaning speed of 45 knots. This effect is shown more clearly in figure 15 where $\frac{\omega_{wet}}{\omega_{dry}}$ values obtained at station F (see fig. 4), a point 352 ft (107.29 m) from wheel entrance into the water trough, for the single-tandem and single wheel configurations (configurations V and VI) are plotted against the velocity ratio $\frac{V_G}{V_P}$. The data shown in this figure suggest that wheel spin-down begins at a speed equivalent to 70 percent of the tire hydroplaning speed V_P. Total spin-down (wheel stops) or maximum spin-down occurs between 80 and 120 percent of the tire hydroplaning speed and further increases in velocity ratio or ground speed result in less wheel spin-down. This latter effect (less wheel spin-down) was noted in references 3 and 5, and it is believed to be the result of: (1) less tire-fluid exposure time in the trough due to the increased ground speed and (2) a more uniform hydrodynamic pressure in the tire-ground contact region under total hydroplaning conditions, which tends to reduce the wheel spin-down moment.

Effect of fluid density.- Figure 16 shows values of the ratio $\frac{\omega_{wet}}{\omega_{dry}}$ obtained for landing-gear wheel configurations III and V at nearly the same ground speeds for two runway fluids, water and slush. It can be seen from this figure that less wheel spin-down occurs in slush than in water for both wheel configurations investigated. The average specific gravity of the slush used in this investigation was approximately 0.88. Hence, the dynamic pressure of slush, if slush acts as a fluid, should be less than dynamic pressure of water and thereby should produce a smaller spin-down moment. This effect is also shown in figure 17 by the data obtained with the single wheel configurations since the wheel spun down more in water than in slush.

Effect of tire pressure.- The effect of tire pressure on wheel spin-down is shown in figure 18. This figure shows the variation of the wheel-angular-velocity ratio $\frac{\omega_{wet}}{\omega_{dry}}$ with ground speed for the single tandem wheels (configuration V) at tire pressures of 25 and 75 lb/in^2 (17.2 and 51.7 N/cm^2). The vertical load $F_{z,g}$ was the same for both pressures. It can be seen that with a tire pressure of 25 lb/in^2 wheel spin-down began at approximately 30 knots and was greatest at approximately 50 knots. With a tire pressure of 75 lb/in^2 spin-down began at about 55 knots and was greatest at about 72 knots. The speed at which spin-down begins with each tire pressure is approximately 70 percent of the hydroplaning speed. It is apparent from these data that increasing the tire pressure increases the speed required for wheel spin-down to begin.

Another effect of tire pressure is indicated by figure 18. The wheel spun down to a complete stop with a tire pressure of 25 lb/in^2 (17.2 N/cm^2) whereas it did not with a

pressure of 75 lb/in^2 (51.7 N/cm^2). This difference could be due to the tire footprint area which, at constant load, increases as the tire pressure is decreased. The larger footprint area with a pressure of 25 lb/in^2 probably produced a larger spin-down moment than that with a pressure of 75 lb/in^2 and thus caused the wheel to spin down to a stop.

Effect of wheel configuration.- The spin-down characteristics in water of each wheel of the diagonal wheels (configuration IV) are shown in figure 19. The data show that neither wheel spun down at ground speeds below the hydroplaning speed of 45 knots. However, at higher ground speeds both wheels spun down with the rear wheel spinning down sooner and to a greater degree. This characteristic is to be expected since, with this wheel arrangement, a wedge of water is present under each wheel and causes the wheel to spin down. The fluid spray from the front wheel impinging on the rear wheel as well as the water in front of the rear wheel being disturbed by the wake of the front wheel probably caused the rear wheel to spin down faster and to a greater degree. In configuration V the wheel arrangement is similar to that of configuration IV except that the rear wheel is mounted directly behind the leading wheel. With this single-tandem wheel arrangement, the rear wheel did not spin down at any test ground speed as shown by figure 16(a). Apparently, the front wheel of this configuration displaced enough water from the path of the rear wheel so that there was not a sufficient amount remaining to cause the rear wheel to spin down.

Effect of vertical load.- At the same tire pressure an increase in the vertical load causes the wheel to spin down to a greater degree. This effect is shown in figure 15. It can be seen that the single wheel with a tire pressure of 75 lb/in^2 (51.7 N/cm^2) spun down to a stop whereas the single tandem wheel did not. The vertical load on the single wheel was about twice that on each wheel of the single-tandem wheel configuration. Consequently, the tire footprint was larger for the single wheel and produced a larger spin-down moment which caused the wheel to come to a complete stop.

Effect of water depth.- Some indication of the effect of water depth on wheel spin-down of each wheel of the dual front wheels (configuration II) with a tire inflation pressure of 25 lb/in^2 (17.2 N/cm^2) is shown in figure 20. The water depth varied from 0.15 to 1.25 in. (0.38 to 3.18 cm) and the ground speed was in the neighborhood of 70 knots, a speed which is well above the approximate hydroplaning speed of 45 knots. The solid curves indicate that the wheels began to spin down as soon as they entered the water but spun up as the water depth decreased. A similar effect is shown by the dashed curves but to a greater degree. At the greater water depths the wheels spun down to a complete stop. These data indicate that for this configuration a water depth of approximately 0.40 in. (1.01 cm) is required to cause wheel spin-down. However, it should be kept in mind that other factors such as tire-tread pattern, runway surface texture, and fluid density may have large effects on the wheel spin-down characteristics. In addition, the

spray pattern and fluid flow developed with this wheel configuration may also affect the wheel spin-down characteristics. Motion pictures taken during the tests show that there is spray and flow interference with this configuration in which two wheels are mounted side by side.

Figure 21 also gives some indication of the effect of water depth on wheel spin-down. The data shown in this figure were obtained during tests with the dual tandem wheels (configuration I) in 0.5 in. (1.27 cm) of water with tire inflation pressures of 50 lb/in^2 (34.5 N/cm^2) and in 2.0 in. (5.08 cm) of water with tire pressures of 75 lb/in^2 (51.7 N/cm^2). In 0.5 in. of water, with a tire pressure of 50 lb/in^2, and at ground speeds near and greater than the hydroplaning speed of 63 knots, the front wheels of this configuration spun down but the rear wheels did not spin down at any speed. However, in 2.0 in. of water, with tire pressures of 75 lb/in^2, and at a ground speed greater than the hydroplaning speed of 78 knots, the rear wheels as well as the front wheels spun down. Evidently, in water of this large depth, the front wheels are raised high enough in the water so that they do not displace all of the water from the path of the rear wheels but leave an appreciable depth for the rear wheels to displace and thereby cause them to spin down.

Wheel Spray Patterns

Motion pictures from the 16-mm and 70-mm cameras provided a means of studying the wheel spray patterns. Figures 22 to 28 show photographs from the 70-mm camera of typical fluid spray patterns attained for the test conditions with the different wheel configurations. In figures 23 to 28, the fluid depth and ground speed are given for each test condition. In addition, the ratio of the ground speed to the predicted hydroplaning speed (determined from eq. (1)) is given. For values of this ratio less than 1.0 the wheel is considered to be in a condition of partial hydroplaning. For velocity-ratio values of 1.0 and greater, the wheel is considered to be in a condition of total hydroplaning.

Types of spray patterns.- The photographs of figures 22 and 23, as well as the 16-mm motion pictures taken during this study, indicate that three distinct types of spray patterns are developed by the dual tandem wheels (configuration I) in slush and water; namely, (1) a bow wave formed at the intersection of the front of the tires with the runway, (2) side waves formed at the intersection of the outboard sides of the dual tires with the runway, and (3) a "rooster tail" or reinforced wave formed by the mixing of two side waves developed on the inboard sides of the dual tires of the landing gear.

Different wheel configurations.- The motion pictures show that this reinforced wave also developed between the tires of the two other dual wheel configurations (configurations II and III). Figure 24(e) shows this wave during a test with configuration II. A spray pattern similar to the rooster tail was also observed on the single-tandem wheel

12

configuration (configuration V) as shown in figures 25(d) and (e). It is believed that this particular spray pattern on the tandem wheel configuration arises from the side spray wave of the front tandem wheel impacting on and being deflected by the exposed rear axle of the landing gear. The large amounts of spray surrounding the dual-tandem wheel configuration prevented observations of the interference spray patterns developed between the wheels of this landing gear. Some assessment of this spray effect can be made by studying the photographs obtained of the diagonal wheels (configuration IV) shown in figure 26. Photographs 26(e) and (f) obtained at the higher ground speeds show that the side wave developed by the front wheel subsequently impinges directly on the opposite mounted rear wheel.

One other interesting wheel-spray-pattern effect was noted. Motion pictures taken of the rear-mounted wheel configurations (configurations III and VII) showed that the bow waves formed on the tires of these configurations could impact with some forward velocity on the rear of the landing-gear structure (strut and front wheel axles) that is ahead of the rear-mounted tires. This spray impingement results in some forward thrust being produced on the landing gear. Photographs illustrating this effect are shown in figures 27 and 28.

The intensity or thickness of the wheel spray developed on all configurations appeared to increase as the fluid depth increased.

Figure 28, which shows photographs of the spray patterns developed by the single-rear wheel configuration, indicates that the spray patterns were about the same shape in slush or in water.

Effect of ground speed on spray patterns.- For all wheel configurations, the angle formed between the bow wave and the ground was quite large at ground speeds below the hydroplaning speed and large amounts of fluid spray were thrown nearly vertically into the air where it subsequently impinged on other parts of the landing gear and test carriage structure. (See figs. 23 and 24.) The maximum height reached by spray from the bow wave was estimated to be about 30 feet. As the ground speed was increased above the critical hydroplaning velocity, the angle between the bow wave and runway decreased progressively until at some high ground speed, the bow wave completely disappeared on the landing gear. The outboard side waves appeared to act in a manner similar to the bow wave just described except that at the higher ground speeds they did not disappear completely but did become much flatter. In contrast with the results observed for the bow and side waves, the rooster tail usually maintained a high angle with respect to the ground over the entire range of ground speeds.

Fluid-Spray Drag on Simulated Wing Flap

References 4 and 5 indicate that minor fluid-spray impingement from the main gear wheels occurred on the wing flaps of the airplane when they were set at the take-off position of 22°. It would be expected that when the flaps were set at the landing position of 55°, more fluid-spray-impingement drag would be experienced on the airplane since the flaps would be closer to the ground and to the landing-gear wheels. Tests were made during this investigation with a simulated flap in the two positions. (See fig. 4.)

The effect of fluid-spray-impingement drag is shown by the curves in figure 29 which were obtained with the single-front wheel configuration (configuration VI). Figure 29(a) shows the upper mass drag to be slightly higher than the landing-gear drag with the flap set at 22°. Apparently some spray impinged on the flap. Since this wheel was more forward of the flap, the spray pattern was high enough to reach the flap. With the flap set at the landing configuration of 55°, an appreciable amount of spray evidently impinges on the flap as shown by the curves in figure 29(b). The maximum drag measured on the upper mass was approximately 70 percent greater than that measured on the landing gear.

Pitching Instability of Bogie Landing Gear

Some tests were made with the dual tandem wheels (configuration I) at a light weight of 12 000 lb (53 378 N) and a tire pressure of 75 lb/in^2 (51.7 N/cm^2) in 1.0 in. (2.54 cm) of water. The landing-gear wheels were free to pitch about the truck-beam pivot since the pitching snubbers had been removed. Under these conditions, the landing gear was very unstable in pitch at speeds near and above the hydroplaning speed. Large pitching oscillations occurred as indicated by the photographs in figure 30. These photographs are frames from a motion picture made during a test in which the ground speed was approximately 100 knots. The oscillations can be seen by noting the relative positions of the instrument covers mounted on the ends of each axle. In frames 17 and 24, the front wheels appear to be completely above the water surface. This pitching instability is believed to be due to hydroplaning. As the front wheels began to hydroplane they rose in the water and therefore less water was removed from the path of the rear wheels. This allowed hydrodynamic forces to act on the rear wheels, raising them and forcing the front wheels down. With the front wheels down and in contact with the water, the hydrodynamic force on the rear wheels was removed and began acting on the front wheels again and the oscillation was repeated. These oscillations were so severe that the wire rope used to prevent the truck beam from rotating to an excessive nose-down attitude when the landing gear was airborne failed.

Fluid-Spray-Drag Alleviator

The large difference in the drag parameter of the dual tandem wheels (configuration I) and the dual front wheels (configuration II) shown in figure 13(a) suggested that the drag due to fluid spray might be reduced by installing a spray shield or alleviator between the dual tandem wheels. Therefore, tests were made with each of three spray alleviators mounted along and under the bogie landing-gear truck beam as shown in the sketches in figure 31. The variation of drag parameter with ground speed obtained with the landing gear equipped with each of the spray alleviators is shown by the solid curve faired through the data whereas the variation obtained without a spray alleviator is shown by the dashed curve. Figures 31(a) and (b) show that the flexible rubber and the rigid metal alleviator increased the maximum drag parameter slightly. However, when the rigid metal alleviator was equipped with a curved top which almost closed the space between the dual wheels (see fig. 10), the maximum drag was reduced approximately 45 percent as shown in figure 31(c). The effectiveness of this alleviator is also shown by comparing the solid curve in figure 31(c), which represents the drag parameter obtained with this spray alleviator, with the curves in figure 13(a). It can be seen that the spray alleviator installed on the dual tandem wheels reduces the maximum drag parameter to a value less than that obtained with the dual front wheels (configuration II). The dual tandem wheels equipped with this spray alleviator is designated as configuration IA in table I. This table shows that installing the spray alleviator on the dual tandem wheels reduced the fluid drag factor from 3.33 to 1.86.

CONCLUSIONS

Ground-run tests were made with a bogie landing gear in water and slush of depths up to 2.0 inches (5.08 centimeters) over a speed range of 15 to 110 knots. Tire inflation pressures of 25, 50, and 75 pounds per inch^2 (17.2, 34.5, and 51.7 newtons per centimeter^2) were used. Wheel configurations consisting of one and two wheels at different locations on the bogie truck as well as the normal four-wheel (dual tandem) configuration were used during the tests. Some tests were made with a simulated wing flap mounted to the rear of the wheels. In addition, tests were made with a spray alleviator mounted between the wheels of the dual-tandem wheel configuration. The results of these tests indicated the following conclusions:

Fluid Drag Parameter

1. Fluid drag increases approximately parabolically with increasing ground speed up to speeds near the hydroplaning speed after which there is a large reduction in drag.

2. Fluid drag appears to be proportional to fluid density and to the width of the tire at the fluid surface up to the hydroplaning speed as predicted in NASA TN D-552.

3. Decreasing the tire inflation pressure reduces the maximum fluid drag but also reduces the ground speed at which tire hydroplaning will occur.

4. From fluid-drag considerations a tandem wheel configuration is preferable to a dual-wheel landing gear.

5. At the same inflation pressure, increasing the vertical load on a tire increases the tire footprint width which causes an increase in the fluid drag.

Wheel Spin-Down

1. Wheel spin-down begins at a ground speed near 70 percent of the tire hydroplaning speed and total spin-down (wheel stops) occurs between 80 and 120 percent of the hydroplaning speed.

2. The wheels spun down less in slush than in water.

3. Decreasing the tire inflation pressure causes the wheel to spin down at a lower ground speed and to a greater degree.

4. The location of the wheels on the bogie landing-gear truck influences the spin-down characteristics of the wheels.

5. At the same tire pressure, increasing the vertical load causes the wheel to spin down to a greater degree.

6. The rear wheels as well as the front wheels of the dual-tandem wheel configuration spun down in 2.0 inches (5.08 centimeters) of water.

Spray Patterns

1. Three distinct types of wheel spray patterns are developed by dual tandem wheels in slush and water; namely, a bow wave, a side wave, and a "rooster tail."

2. The intensity or thickness of the spray patterns appeared to increase as the runway fluid depth increased.

3. The angle between the runway and the bow wave (and side wave) decreases as the ground speed increases. However, the angle of the rooster tail with respect to the runway appeared to change very little over the entire range of forward speeds.

Fluid Drag on Wing Flap

1. With the single-front wheel configuration, drag due to spray impingement on a simulated wing flap was much higher with the flap in the landing position (55°) than in the take-off position (22°).

2. Fluid spray impinging on the simulated wing flap in the landing position produced a maximum drag on the upper mass which was approximately 70 percent greater than that measured on the landing gear.

Pitching Instability of Bogie Landing Gear

1. For a bogie landing gear undamped in pitch, a severe pitching oscillation due to hydroplaning can develop under certain combinations of tire inflation pressures and vertical load which produce small tire deflections.

Fluid-Spray-Drag Alleviator

1. A fluid-spray-drag alleviator installed between the dual tandem wheels reduced the total maximum fluid drag approximately 45 percent.
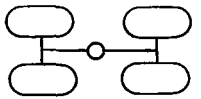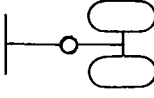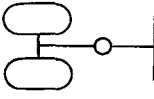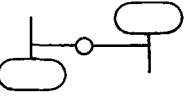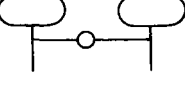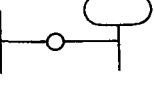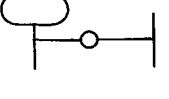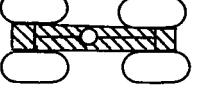
Langley Research Center,
    National Aeronautics and Space Administration,
        Langley Station, Hampton, Va., March 10, 1966.

REFERENCES

1. Horne, Walter B.; Joyner, Upshur T.; and Leland, Trafford J. W.: Studies of the Retardation Force Developed on an Aircraft Tire Rolling in Slush or Water. NASA TN D-552, 1960.

2. Sparks, Allan R.: Report on Effect of Slush on Ground Run Distance to Lift-Off. Doc. No. D6-5198, Boeing Airplane Co., Jan. 1960.

3. Anon.: Joint Technical Conference on Slush Drag and Braking Problems. FAA and NASA, Dec. 1961.

4. Shrager, Jack J.: Vehicular Measurements of Effective Runway Friction. Final Report, Project No. 308-3X (Amendment No. 1), FAA, May 1962.

5. Sommers, Daniel E.; Marcy, John F.; Klueg, Eugene P.; and Conley, Don W.: Runway Slush Effects on the Takeoff of a Jet Transport. Final Report, Project No. 308-3X, FAA, May 1962.

6. Mechtly, E. A.: The International System of Units — Physical Constants and Conversion Factors. NASA SP-7012, 1964.

7. Joyner, Upshur T.; Horne, Walter B.; and Leland, Trafford J. W.: Investigations on the Ground Performance of Aircraft Relating to Wet Runway Braking and Slush Drag. AGARD Rept. 429, Jan. 1963.

8. Horne, Walter B.; and Dreher, Robert C.: Phenomena of Pneumatic Tire Hydroplaning. NASA TN D-2056, 1963.

9. Horne, Walter B.; and Leland, Trafford J. W.: Influence of Tire Tread Pattern and Runway Surface Condition on Braking Friction and Rolling Resistance of a Modern Aircraft Tire. NASA TN D-1376, 1962.

10. Collar, A. R.: On the Drag Due to Slush. Aeronautical Research Council 22,491, E. P. 675, CN 644, Jan. 9, 1961.

11. Anon.: Hazards of Tire Hydroplaning to Aircraft Operation. NASA Langley Research Center Film Serial No. L-775, 1963.

TABLE I.- WHEEL CONFIGURATIONS TESTED AND FLUID DRAG FACTORS OBTAINED

$$\left[p = 75 \text{ lb/in}^2 \text{ (51.7 N/cm}^2\text{)}; \quad d_1 \approx 1.0 \text{ in. (2.54 cm)}\right]$$

Number	Number of wheels	Configuration		Approximate load per tire, lb (N)	Fluid drag factor at maximum drag
		Description	Schematic Direction of motion →		
I	4	Dual tandem		Front: 5 125 (22 797) Rear: 6 025 (26 800) Total: 22 300 (99 195)	3.33
II	2	Dual front		Each: 6 000 (26 689) Total: 12 000 (53 378)	2.04
III	2	Dual rear		Each: 6 000 (26 689) Total: 12 000 (53 378)	1.59
IV	2	Diagonal		Front: 5 520 (24 554) Rear: 6 480 (28 824) Total: 12 000 (53 378)	2.66
V	2	Single tandem		Front: 5 520 (24 554) Rear: 6 480 (28 824) Total: 12 000 (53 378)	1.15
VI	1	Single front		12 000 (53 378)	1.08
VII	1	Single rear		12 000 (53 378)	1.00
IA	4	Dual tandem with fluid-spray-drag alleviator		Front: 5 125 (22 797) Rear: 6 025 (26 800) Total: 22 300 (99 195)	1.86
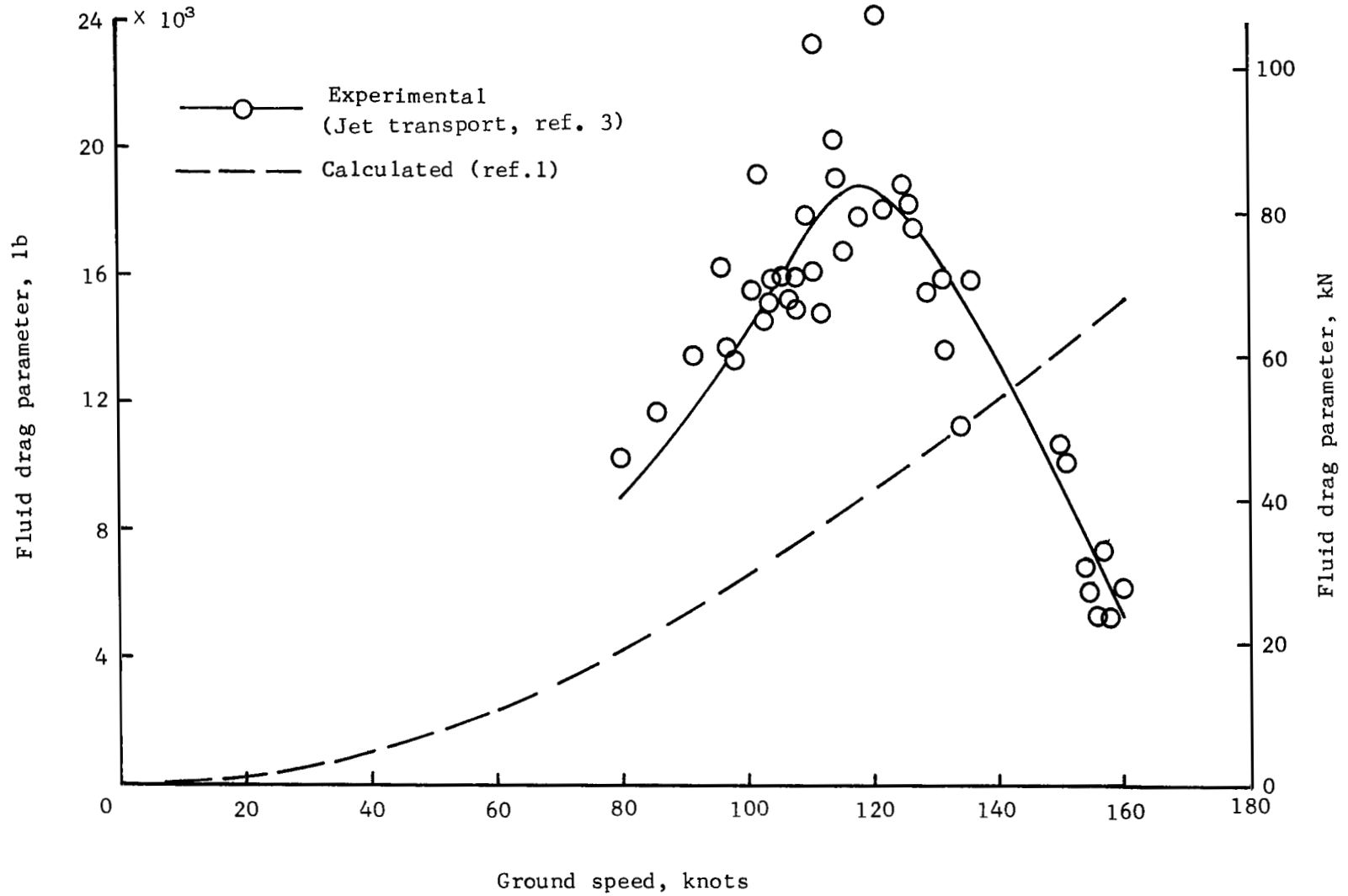
Figure 1.- Comparison of slush drag measured on jet-transport airplane (ref. 3) with drag predicted by means of single-wheel method of reference 1.
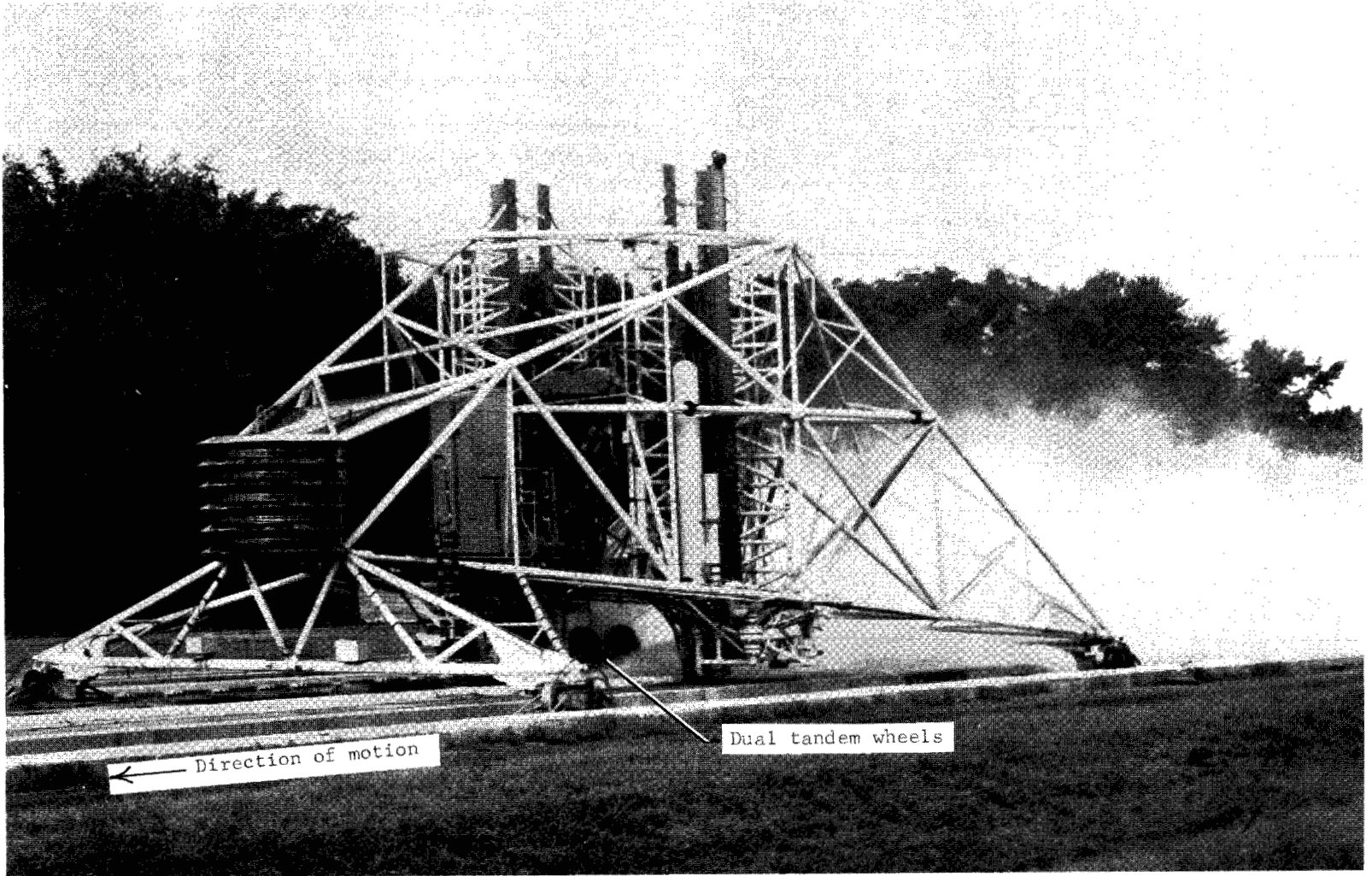
Figure 2.- Test vehicle of Langley landing-loads track.

L-62-1048.1

21

Upper mass drag dynamometer

29.75 in.
75.5 cm

65.28 in.
165.8 cm

8 in. (20.3 cm)
diameter bar

Bogie drag
load cell

Forward ⟶

Truck carriage
beam

Beam pivot

Runway surface

21.6 in.
54.9 cm

25.4 in.
64.5 cm

47 in.
119.4 cm
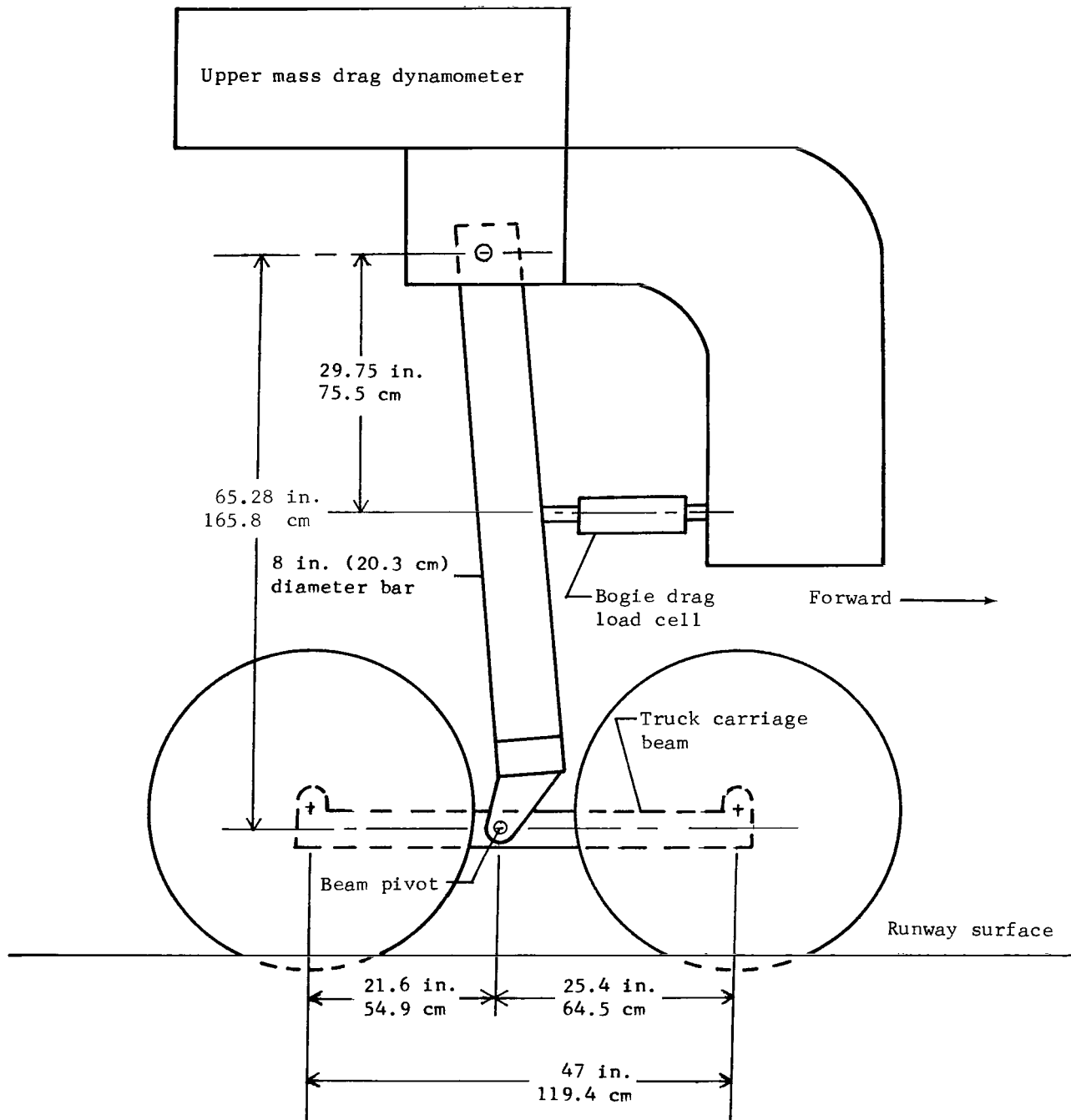
Static vertical load on front axle = 0.46 $F_{z,g}$

Static vertical load on rear axle = 0.54 $F_{z,g}$

Figure 3.- Schematic drawing of dual-tandem landing gear used in tests.

512 ft
156.06 m

Dike

9 ft
2.74 m

Forward ⟶

Dam

A   B   C   D   E   F   G   H

|←32 ft→|←— 64 ft —→|←— 64 ft —→|←— 64 ft —→|←— 64 ft —→|←— 64 ft —→|←— 64 ft —→|←— 64 ft —→|←32 ft→|
9.75 m   19.51 m   19.51 m   19.51 m   19.51 m   19.51 m   19.51 m   19.51 m   9.75 m
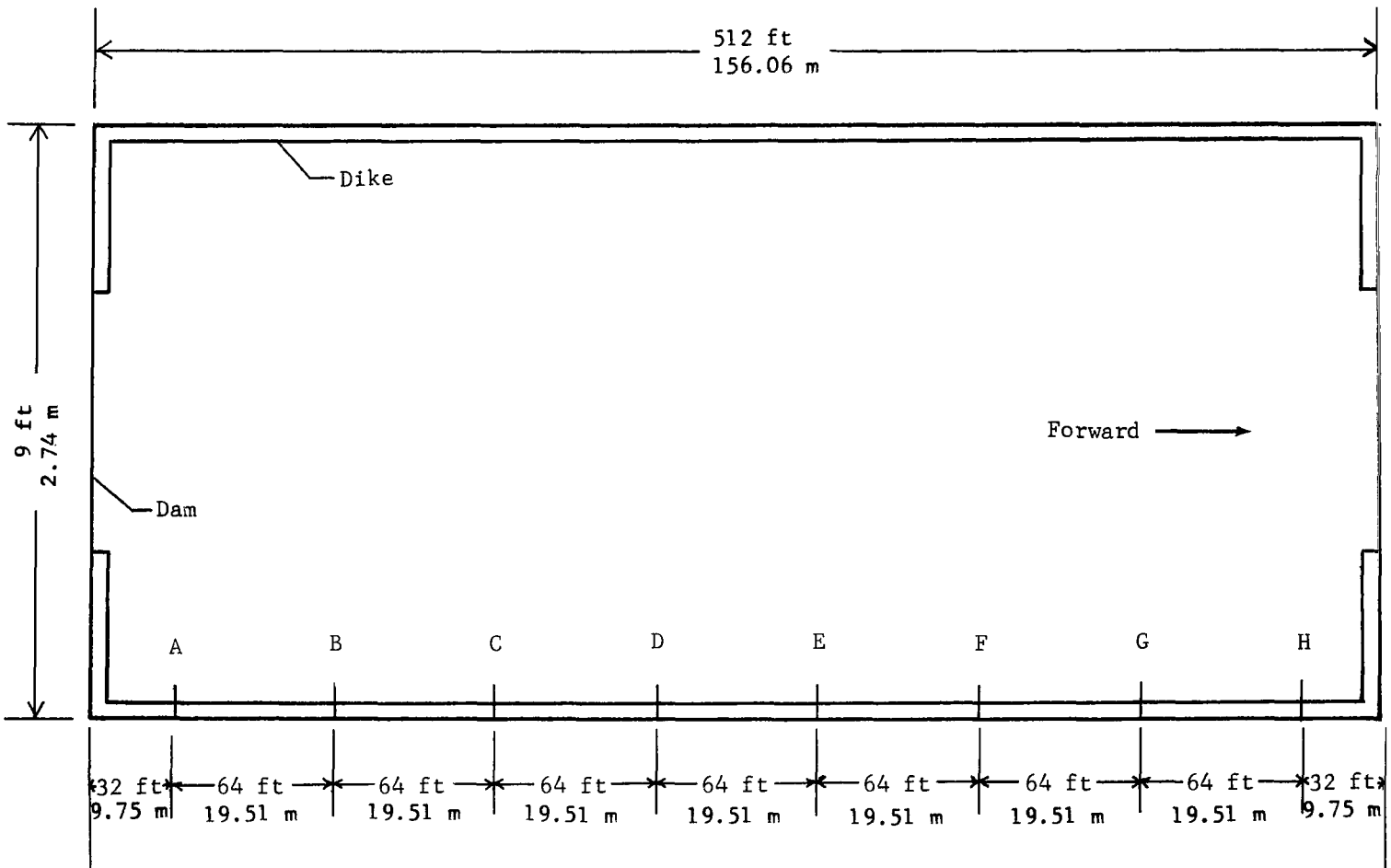
Figure 4.- Sketch of slush and water trough, showing stations at which slush and water depths
were measured.
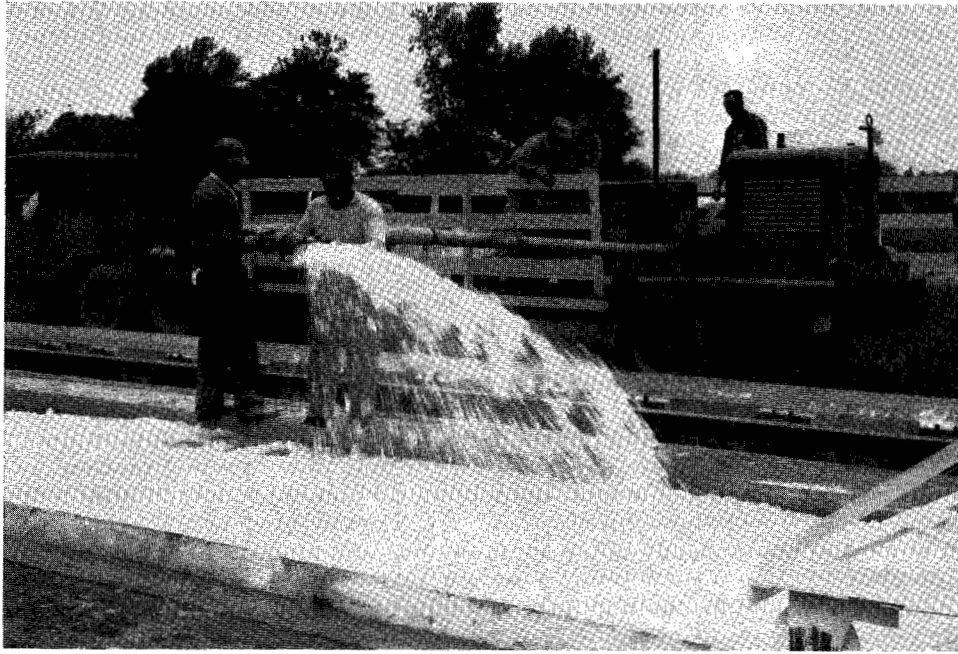
L-66-1179

Figure 5.- Ice-crushing machine used to make slush in operation.
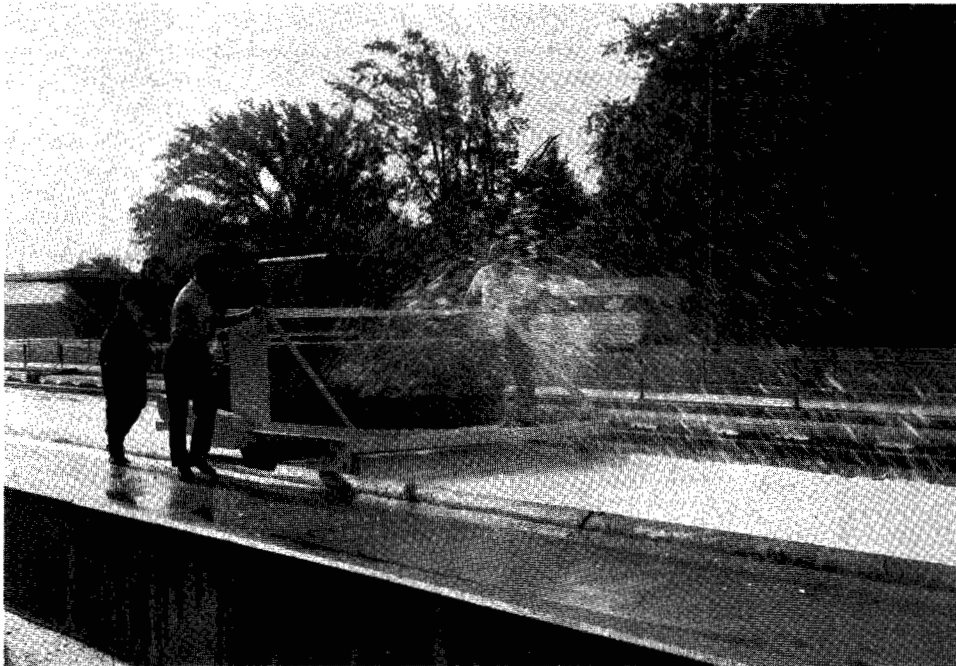
L-66-1180

Figure 6.- Slush-leveling machine used to trim slush to desired test
depth.

24
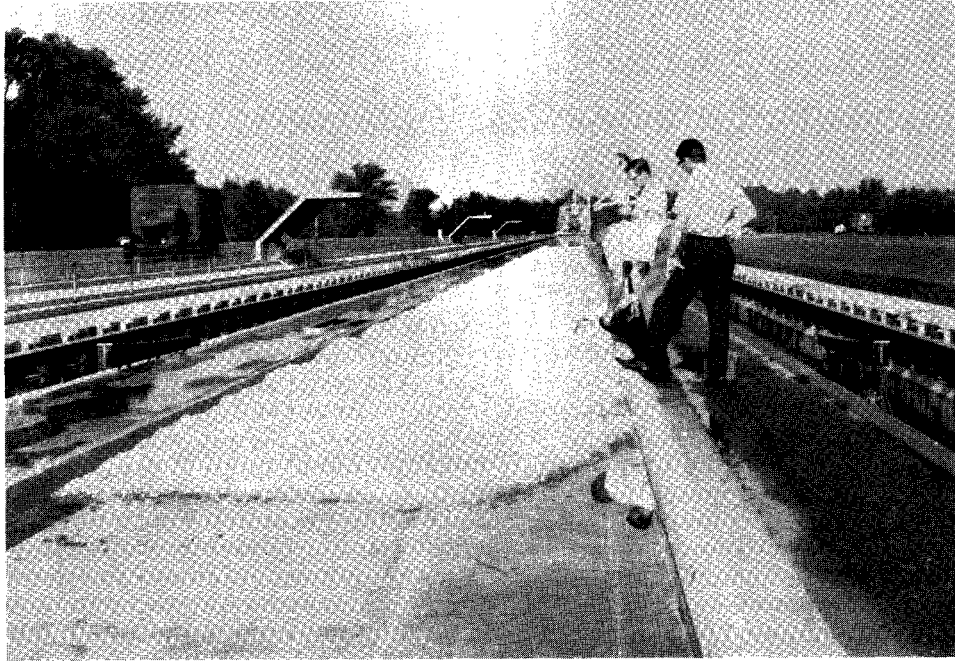
Figure 7.- Slush bed before test.   L-66-1181
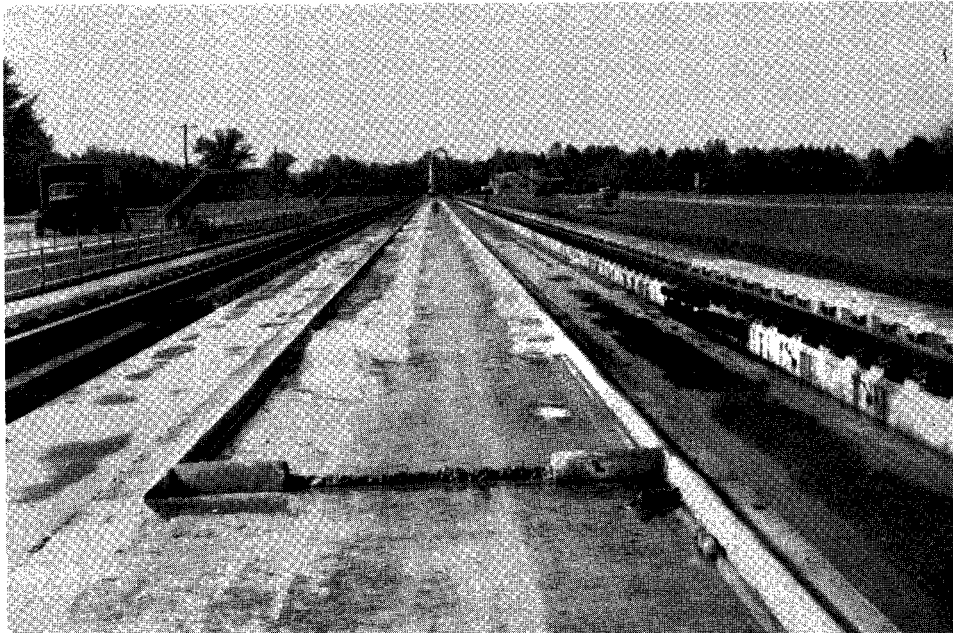
Figure 8.- Slush bed after typical test.   L-66-1182

25

Upper mass drag dynamometer

22°

55°

Flap length = 14.29 ft
4.35 m
Flap width = 4.21 ft
1.28 m

4.79 ft
1.46 m

6.68 ft
2.04 m

4.52 ft
1.38 m

2.93 ft
0.89 m

Forward ⟶

Runway surface
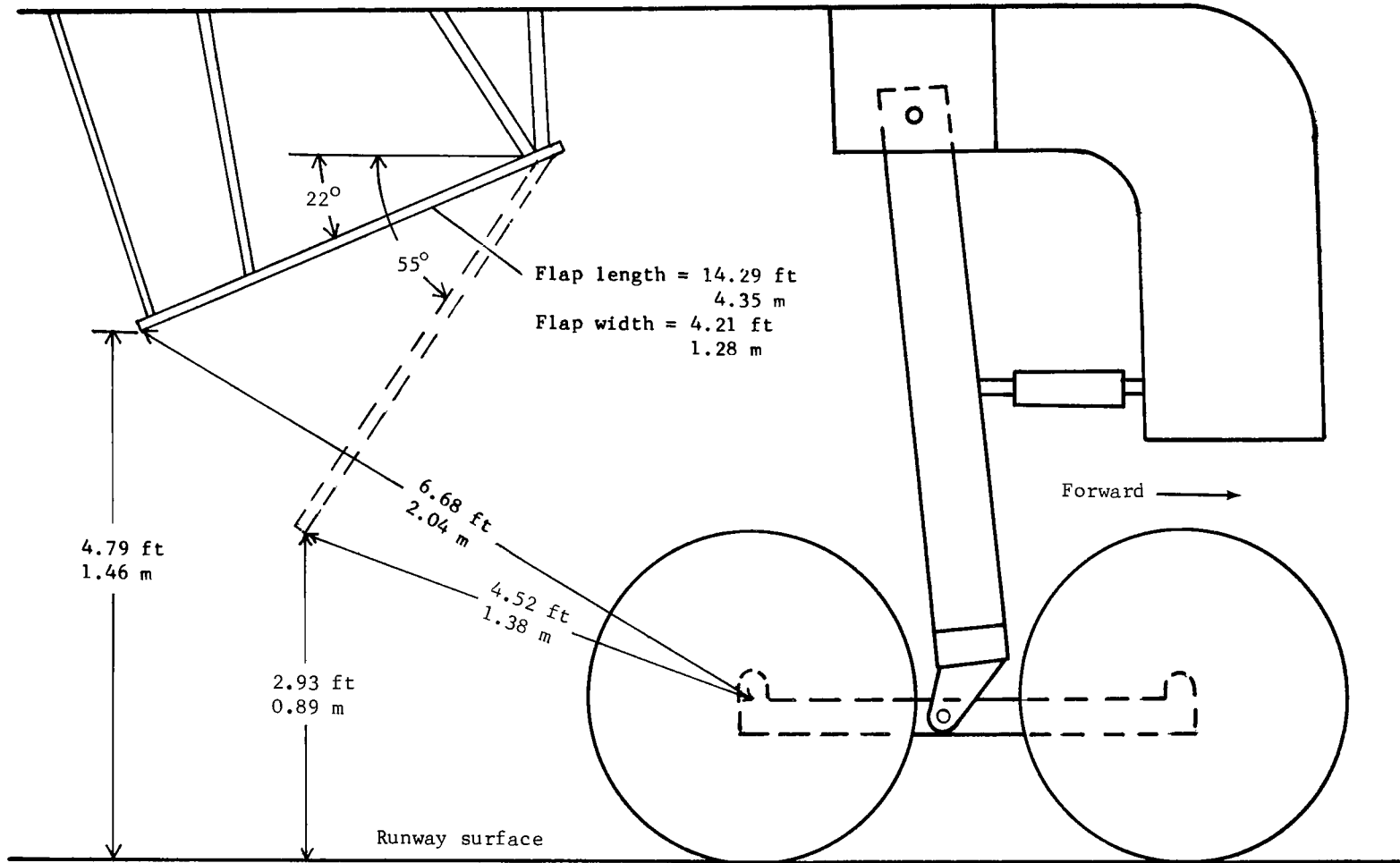
Figure 9.- Schematic drawing of dual-tandem landing gear, showing relative positions of
simulated wing flap.
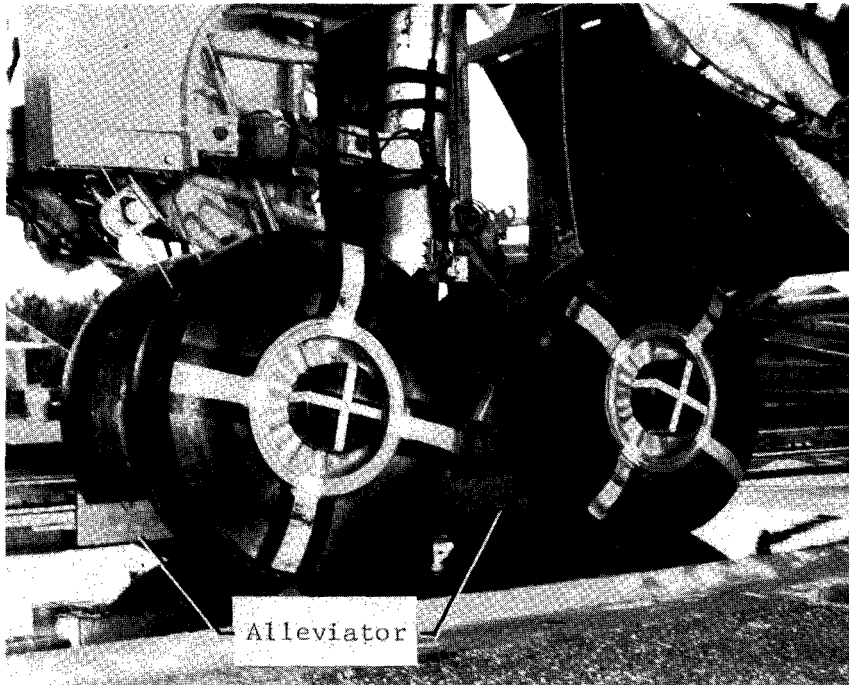
(a) Side view.
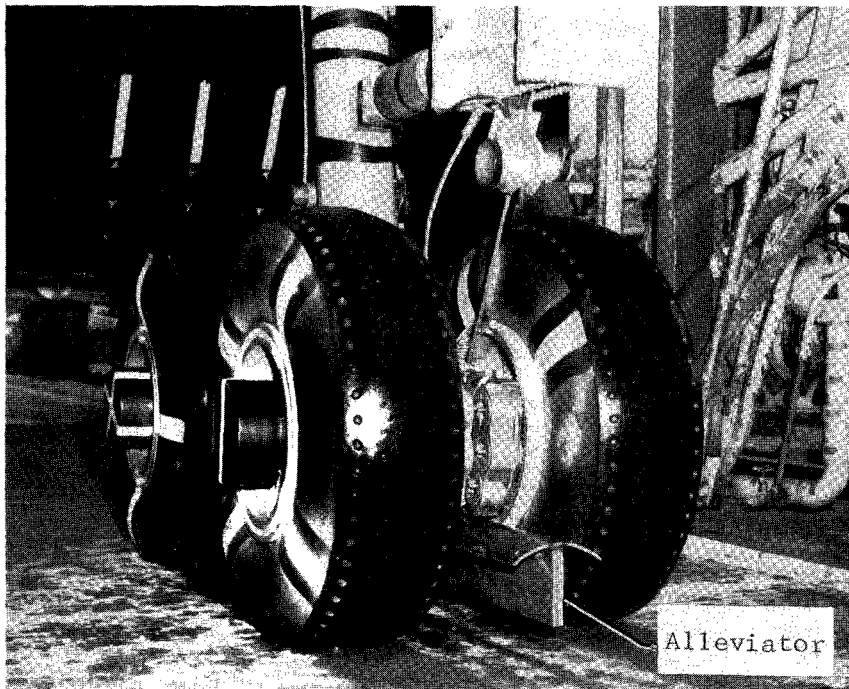
(b) Front view.   L-66-1183

Figure 10.- Spray-drag alleviator mounted on dual tandem wheels
(configuration IA).
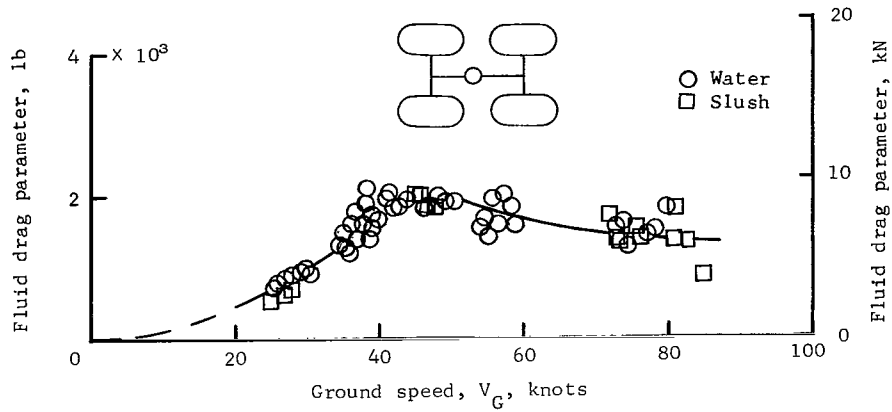
(a) p = 25 lb/in^2 (17.2 N/cm^2).
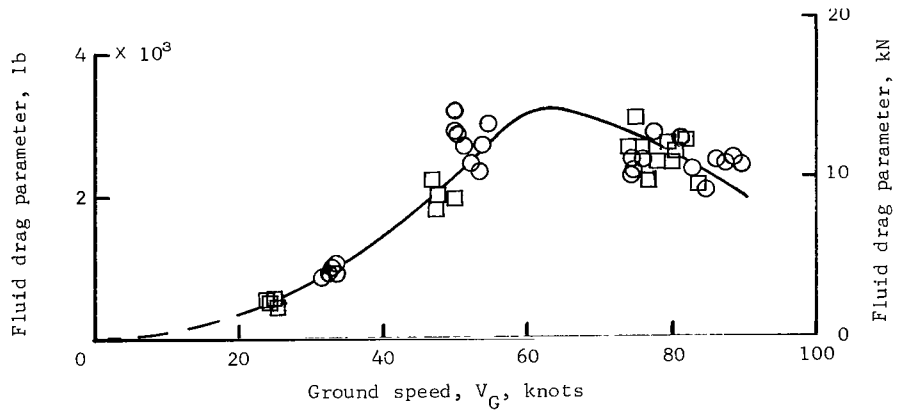
(b) p = 50 lb/in^2 (34.5 N/cm^2).
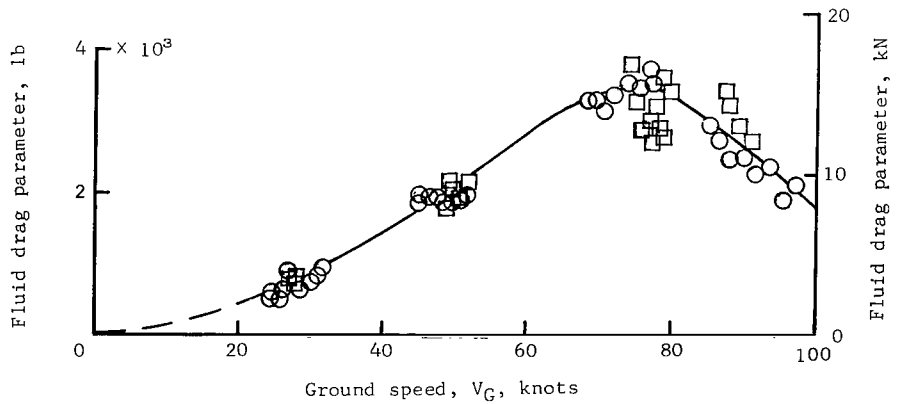
(c) p = 75 lb/in^2 (51.7 N/cm^2).

Figure 11.- Variation of drag parameter with ground speed for dual
tandem wheels (configuration I) in water and slush.
$F_{z,g} \approx 22\ 300$ lb (99 195 N); $d_l = 0.5$ to 2.0 in. (1.27 to
5.08 cm).

Tire pressure, p, lb/in^2 (N/cm^2)	Tire width, b_s, in. (cm)
25 (17.2)	12.0 (30.5)
50 (34.5)	10.8 (27.4)
75 (51.7)	10.1 (25.6)

Drag parameter, D_s $\dfrac{d_{st}}{d_l \times sp. \ gr.}$, lb

Drag parameter, D_s $\dfrac{d_{st}}{d_l \times sp. \ gr.}$, kN

Ground speed, V_G, knots
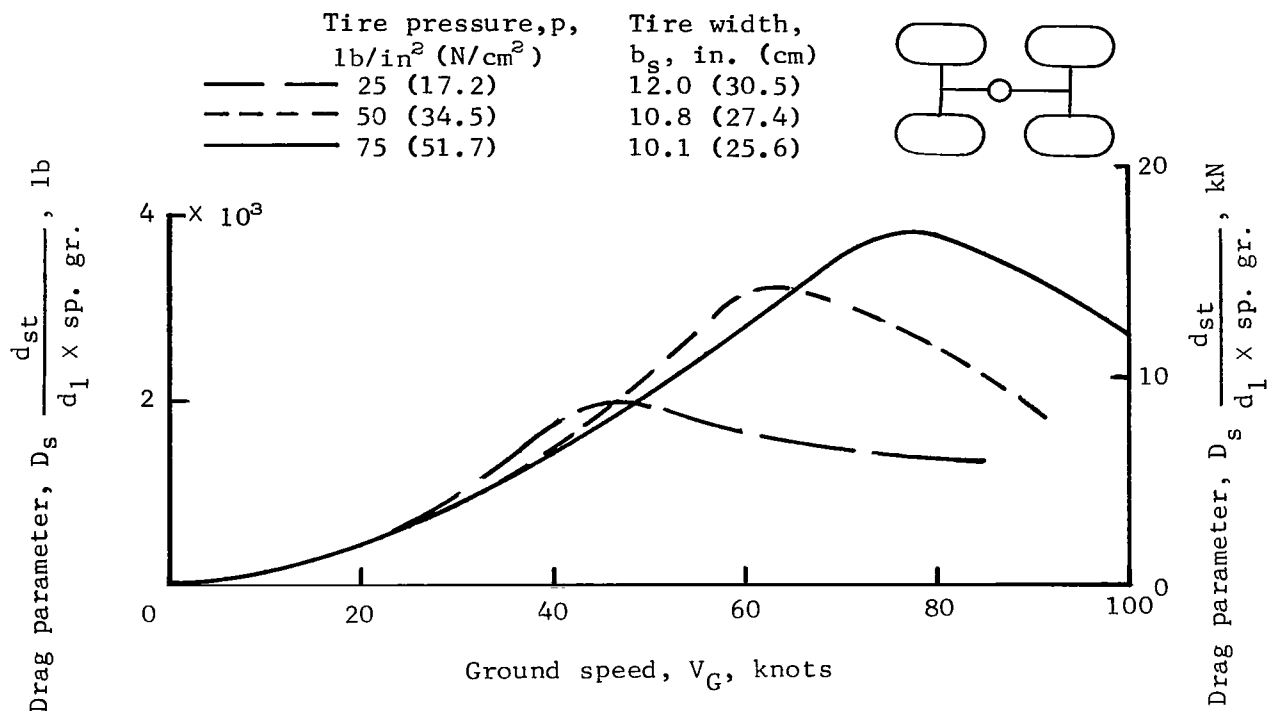
(a) Drag parameter in terms of tire pressure, with tire width not considered.

$b_{st} = 10.1$ in. (25.6 cm)

Drag parameter $\times \dfrac{b_{st}}{b_s}$, lb

Drag parameter $\times \dfrac{b_{st}}{b_s}$, kN

Ground speed, V_G, knots
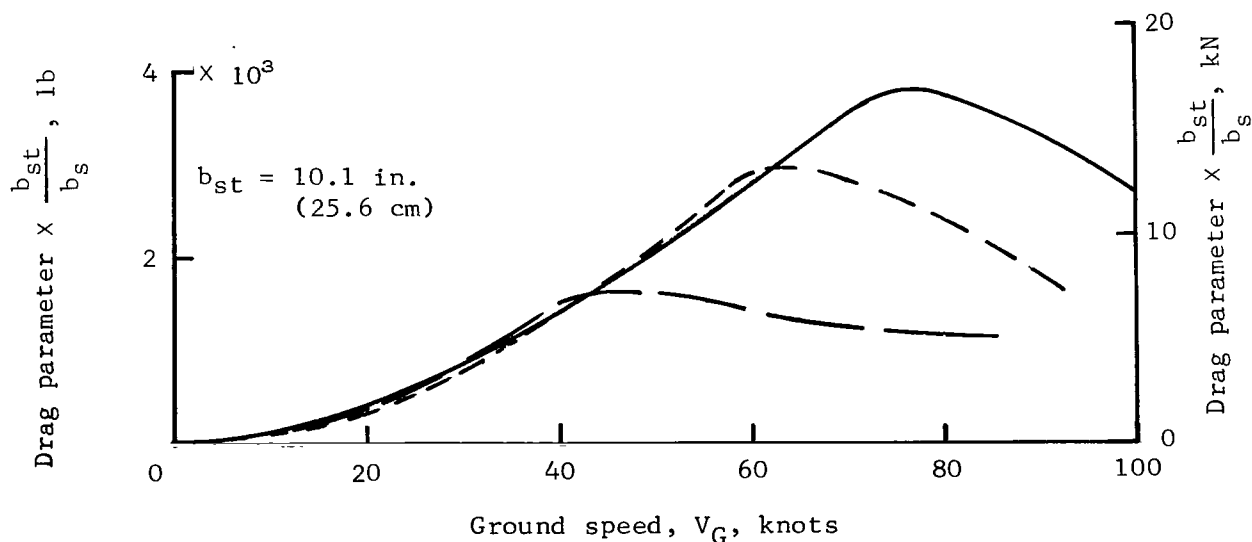
(b) Drag parameter in terms of tire width at 75 lb/in^2 (51.7 N/cm^2).

Figure 12.- Effect of tire width and tire inflation pressure on drag parameter for dual tandem wheels (configuration I).

Approximate load per tire

	Configuration	lb		N	
		Front	Rear	Front	Rear
———————————— I	Dual tandem wheels	5 125	6 025	22 797	26 800
———————————— IV	Diagonal wheels	5 520	6 480	24 554	28 824
———————————— II	Dual front wheels	6 000		26 689	
———————————— III	Dual rear wheels		6 000		26 689
———————————— VII	Single rear wheel		12 000		53 378
———————————— VI	Single front wheel	12 000		53 378	
———————————— V	Single tandem wheels	5 520	6 480	24 554	28 824
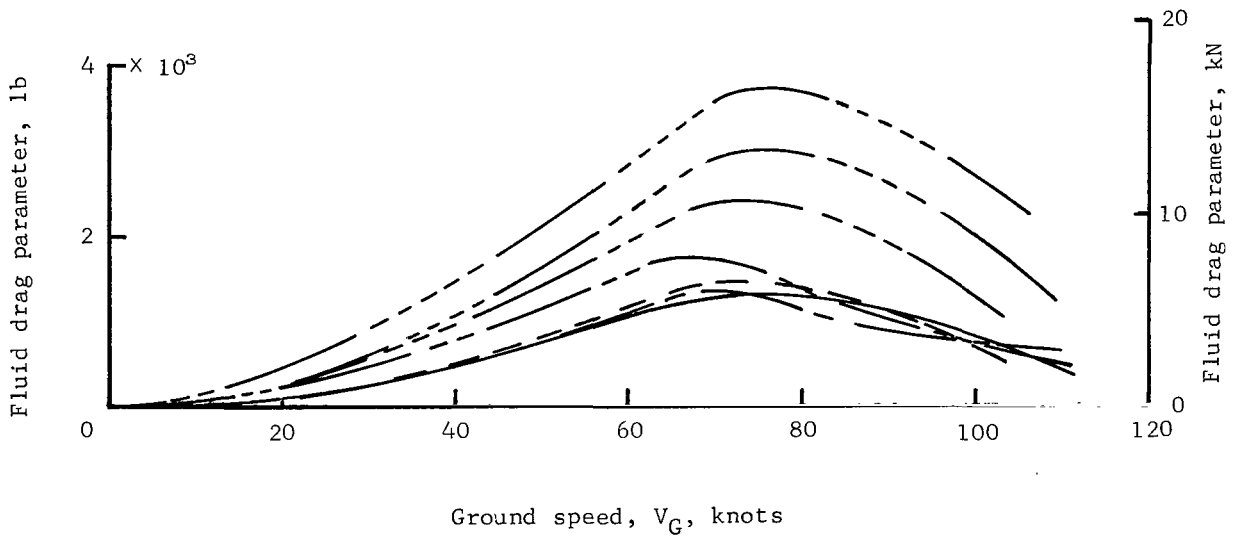
(a) $p = 75$ lb/in^2 (51.7 N/cm^2).
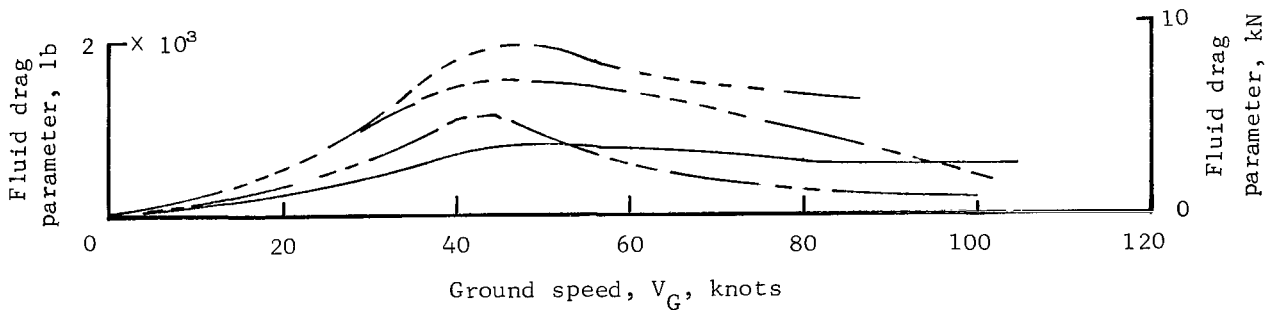
(b) $p = 25$ lb/in^2 (17.2 N/cm^2).

Figure 13.- Variation of drag parameter with ground speed for wheel
configurations on water- and slush-covered runway.
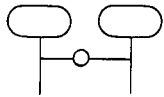
Ground speed range, knots

Single tandem		Dual
23 to 19		24 to 20
33 to 30		31 to 26
		43 to 37
45 to 41		
56 to 50		55 to 48
63 to 55		73 to 64
83 to 78		85 to 74
108 to 101		106 to 92
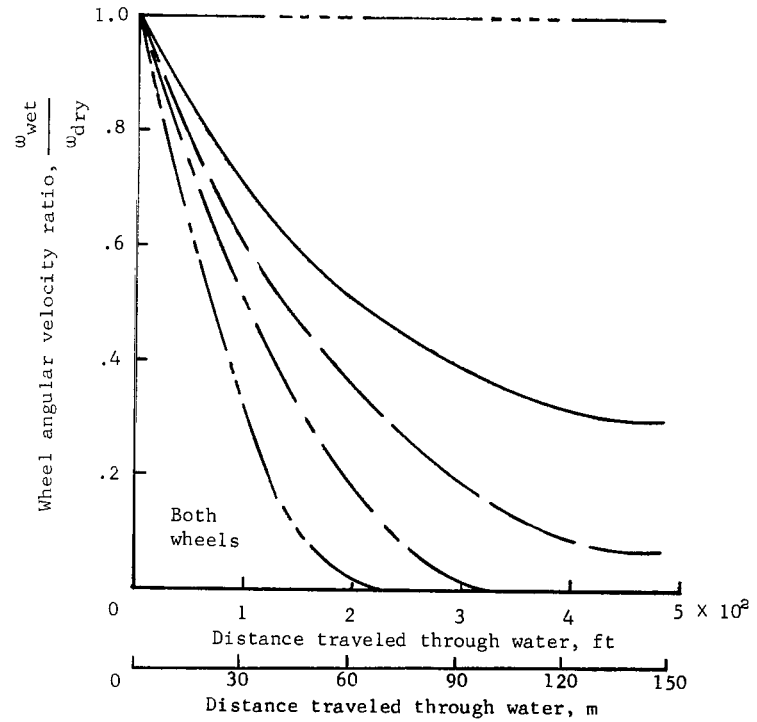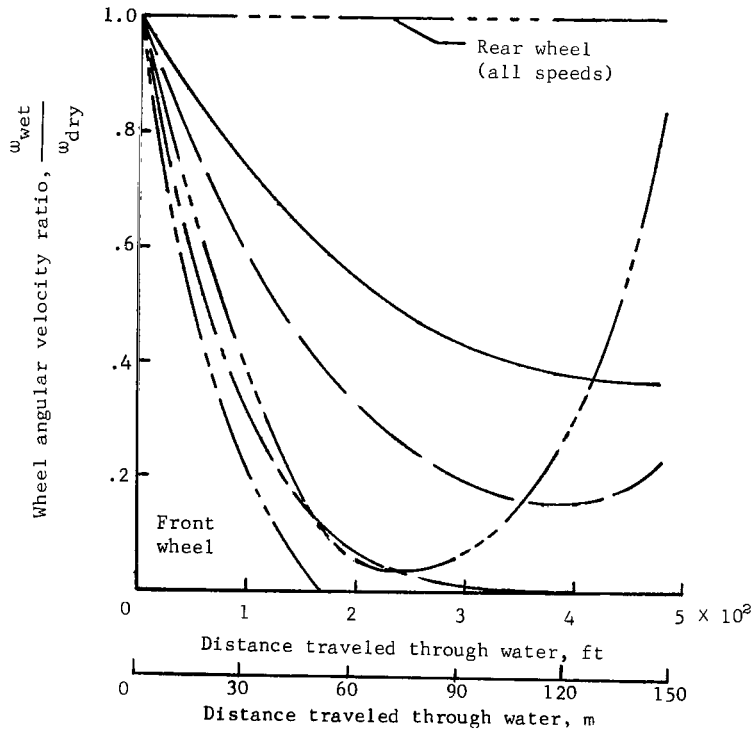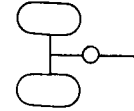
(a) Single tandem wheels (configuration V).   (b) Dual rear wheels (configuration III).

Figure 14.- Spin-down characteristics of single tandem wheels and dual rear wheels in water. $p = 25$ lb/in^2 (17.2 N/cm^2); $F_{z,g} \approx 12\ 000$ lb (53 378 N); $d_1 \approx 1.0$ in. (2.54 cm).

Tire pressure, p,
lb/in^2 (N/cm^2)

——————— 25 (17.2) front wheel
— — 75 (51.7) front wheel } Single tandem wheels
— ———— 25,75 (17.2,51.7) rear wheel } (configuration V)
— — ——— 75 (51.7) single wheel (configuration VI)
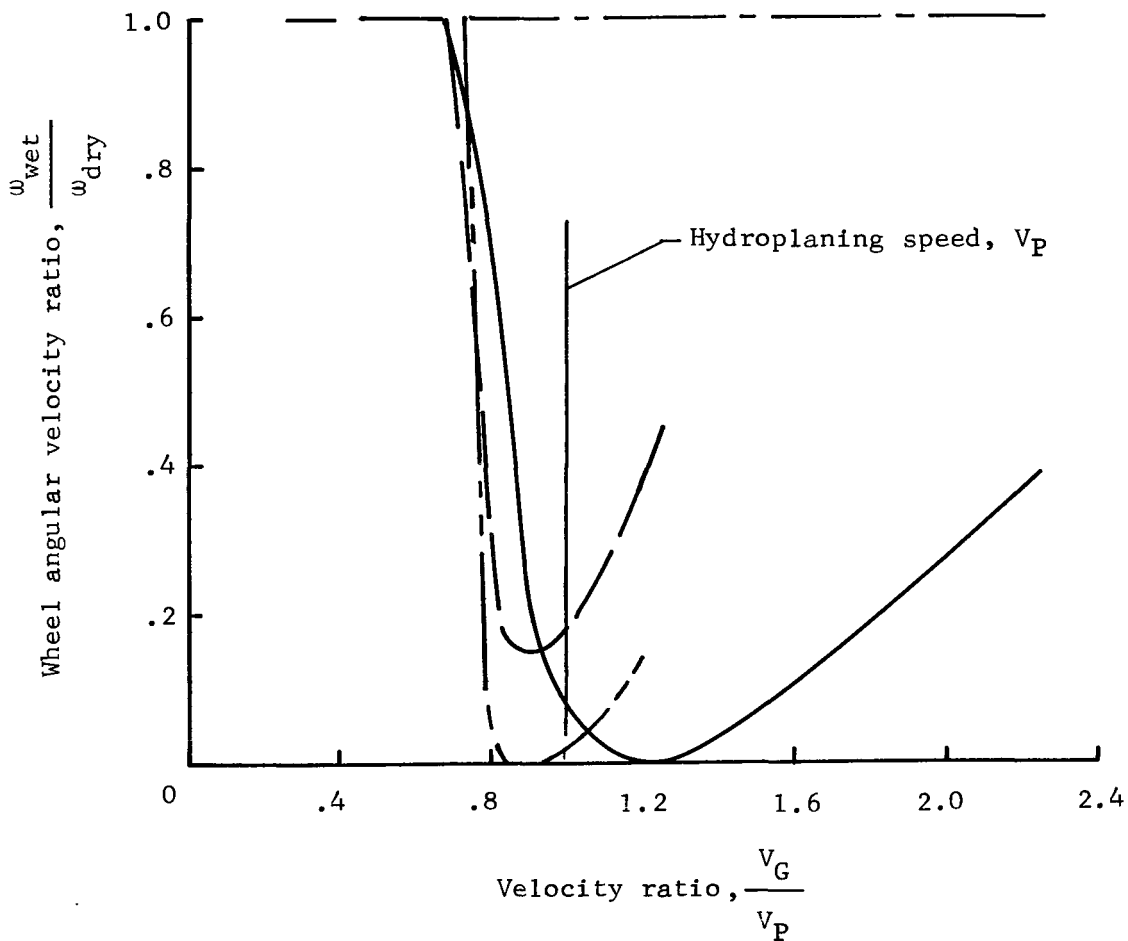
Figure 15.- Variation of wheel angular velocity ratio with velocity
ratio for single tandem and single wheel configurations.

Ground speed range, knots

	Single tandem		Dual rear	
	Water	Slush	Water	Slush
— · —	58 to 52	53 to 47	47 to 41	55 to 48
— —	80 to 72	78 to 71	79 to 67	85 to 73
———	106 to 98	107 to 101	105 to 97	106 to 93

Rear wheel, water and slush (all speeds)

Slush

Water

Front wheel

Wheel angular velocity ratio, $\frac{\omega_{wet}}{\omega_{dry}}$

Distance traveled through fluid, ft

Distance traveled through fluid, m

Slush

Water

Right and left wheel

Wheel angular velocity ratio, $\frac{\omega_{wet}}{\omega_{dry}}$

Distance traveled through fluid, ft

Distance traveled through fluid, m

(a) Single tandem wheels (configuration V).   (b) Dual rear wheels (configuration III).

Figure 16.- Effect of fluid density on spin-down characteristics of single tandem and dual rear wheel configurations. $p = 75$ lb/in^2 (51.7 N/cm^2); $F_{z,g} \approx 12\ 000$ lb (53 378 N); $d_1 \approx 1.0$ in. (2.54 cm).

33

Ground speed range, knots

	Water	Slush
– – – – { 17 to 15 through 64 to 54	17 to 15 through 64 to 54	29 to 25 51 to 46
— – – –	68 to 61	
— — –	81 to 74	
— – —	84 to 78	
— — —	96 to 90	76 to 70
———	99 to 91	100 to 96
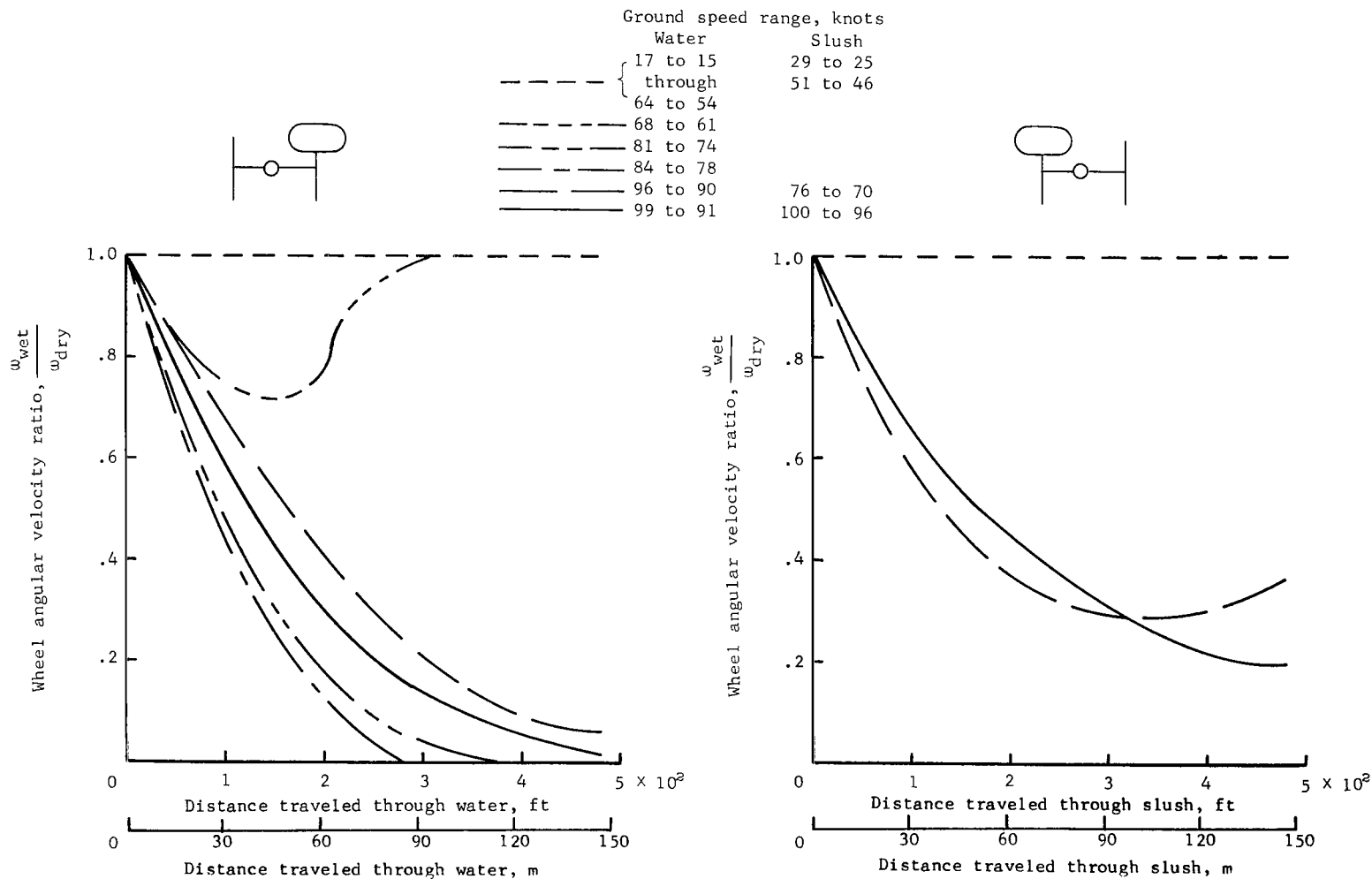
(a) Single front wheel (configuration II) in water.

(b) Single rear wheel (configuration VII) in slush.

Figure 17.- Comparison of wheel spin-down characteristics of single wheel configurations in water and slush. $p = 75$ lb/in^2 (51.7 N/cm^2); $F_{z,g} \approx 12\ 000$ lb (53 378 N); $d_1 \approx 1.0$ in. (2.54 cm).
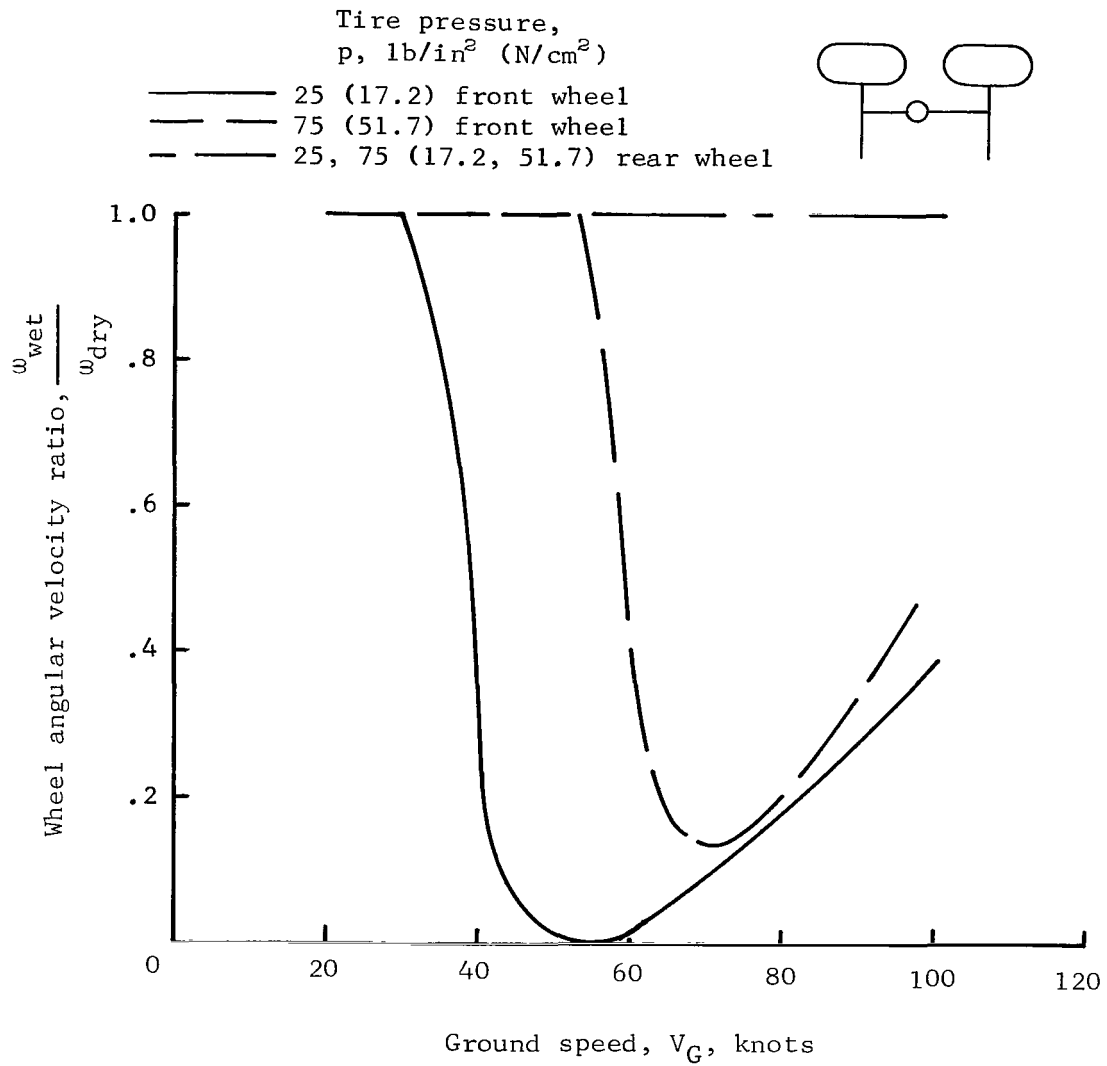
Figure 18.- Effect of tire pressure on wheel spin-down of single tandem
wheels (configuration V).

Ground speed range, knots

28 to 23
32 to 27
42 to 36
60 to 52
65 to 58
68 to 61
85 to 78
109 to 100

1.0

.8

.6

$\dfrac{\omega_{wet}}{\omega_{dry}}$ Wheel angular velocity ratio,

.4

.2

0   1   2   3   4   5 × 10²

Distance traveled through water, ft

0   30   60   90   120   150

Distance traveled through water, m

(a) Left front wheel.

1.0

.8

.6

$\dfrac{\omega_{wet}}{\omega_{dry}}$ Wheel angular velocity ratio,

.4

.2

0   1   2   3   4   5 × 10²

Distance traveled through water, ft

0   30   60   90   120   150

Distance traveled through water, m

(b) Right rear wheel.

Figure 19.- Comparison of wheel spin-down characteristics of left front and right rear wheels of diagonal wheels (configuration IV). $p = 25$ lb/in^2 (17.2 N/cm^2); $F_{z,g} \approx$ 12 000 lb (53 378 N); $d_l \approx$ 1.0 in. (2.54 cm).

Water depth, in. (cm) | Ground speed range, knots
1.25 to 0.80 (3.18 to 2.03) | 71 to 63
1.10 to 0.75 (2.79 to 1.90) | 70 to 62
1.00 to 0.40 (2.54 to 1.01) | 71 to 63
0.45 to 0.15 (1.14 to 0.38) | 68 to 64

Decreasing water depth ——→

Wheel angular velocity ratio, $\dfrac{\omega_{wet}}{\omega_{dry}}$

Distance traveled through water, ft

Distance traveled through water, m
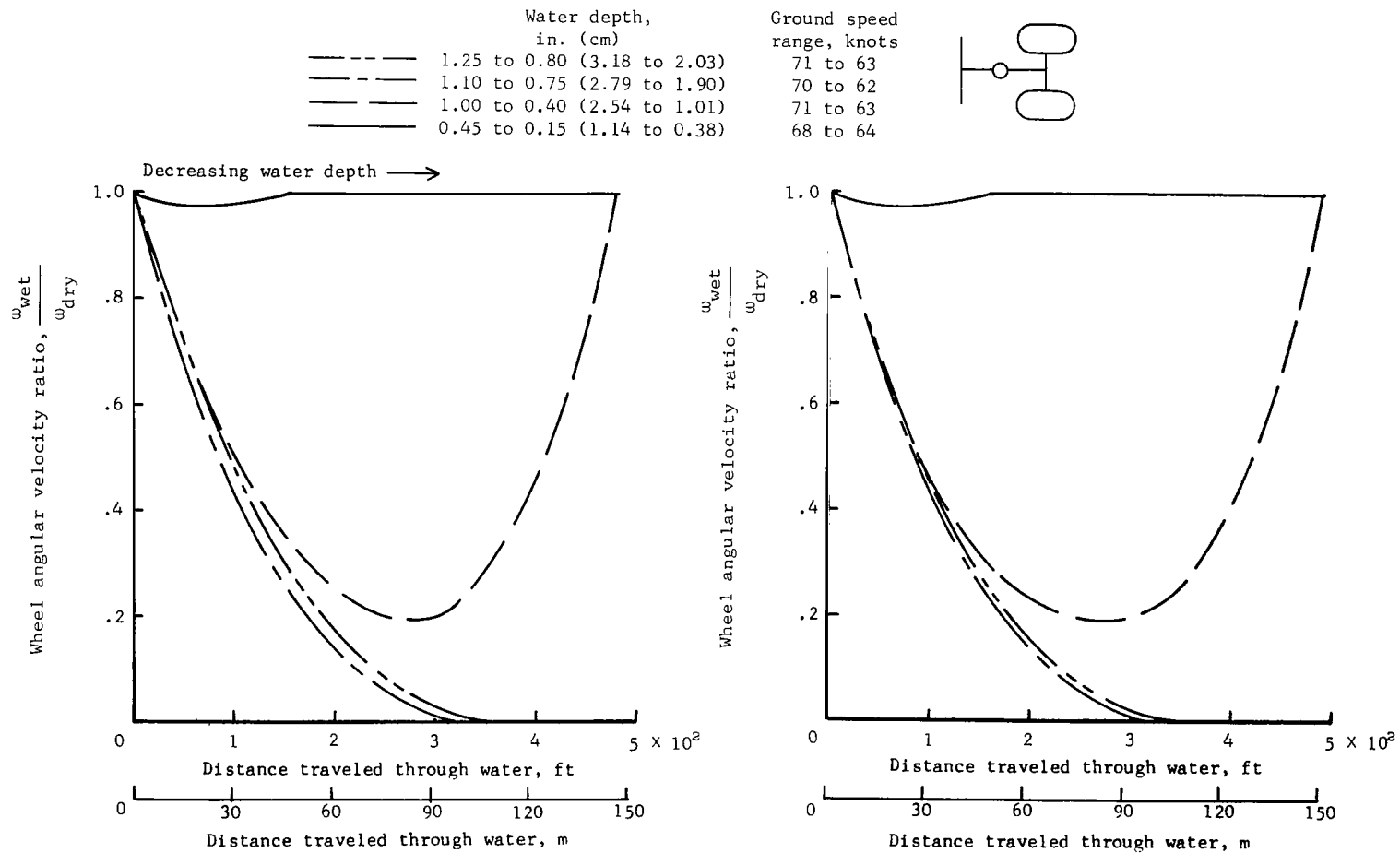
(a) Left wheel.

(b) Right wheel.

Figure 20.- Effect of water depth on wheel spin-down characteristics of front dual wheels (configuration II). $p = 25$ lb/in^2 (17.2 N/cm^2); $F_{z,g} \approx 12\,000$ lb (53 378 N).

Ground speed range, knots
—— · —— { 33 to 28
             { 52 to 45
——————— 97 to 85

Ground speed range, knots
——— – ——— 35 to 31
——————— 55 to 50
——————— 91 to 83

Wheel angular velocity ratio, $\dfrac{\omega_{wet}}{\omega_{dry}}$

1.0

.8

.6

.4

.2

Front and
rear wheels

Right rear wheel

Front wheels

Left rear wheel

0   1   2   3   4   5 × 10²

Distance traveled through water, ft

0   30   60   90   120   150

Distance traveled through water, m

Wheel angular velocity ratio, $\dfrac{\omega_{wet}}{\omega_{dry}}$

1.0

.8

.6

.4

.2

Front wheels
Rear wheels (all speeds)

Front wheels

0   1   2   3   4   5 × 10²

Distance traveled through water, ft

0   30   60   90   120   150

Distance traveled through water, m

(a) Water depth ≈ 2.0 in. (5.08 cm);
    p = 75 lb/in² (51.7 N/cm²).

(b) Water depth ≈ 0.5 in. (1.27 cm);
    p = 50 lb/in² (34.5 N/cm²).

Figure 21.- Comparison of wheel spin-down characteristics of front and rear wheels of dual tandem
wheels (configuration I) in water. $F_{z,g} \approx$ 22 300 lb (99 195 N).
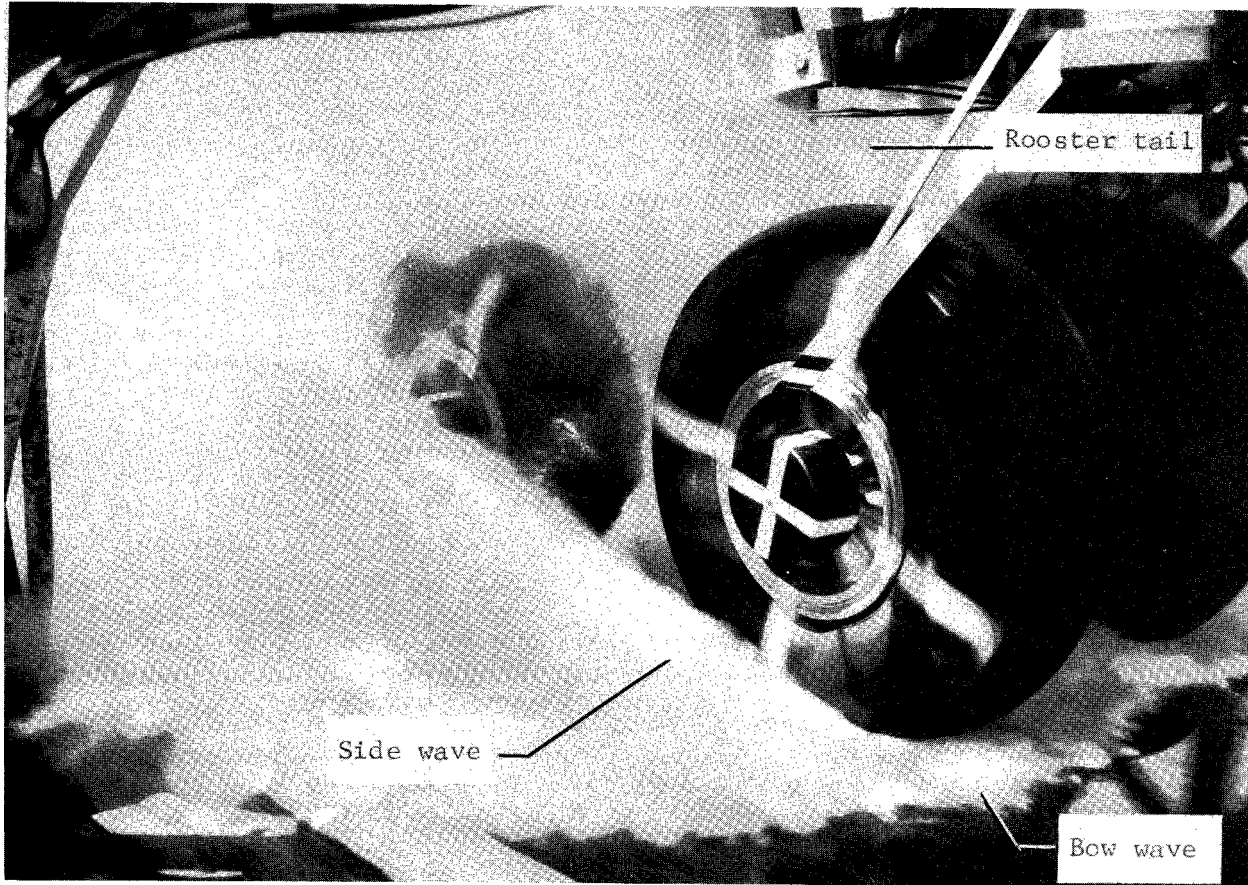
L-66-1184
Figure 22.- Typical fluid spray patterns developed on dual tandem
wheels (configuration I).
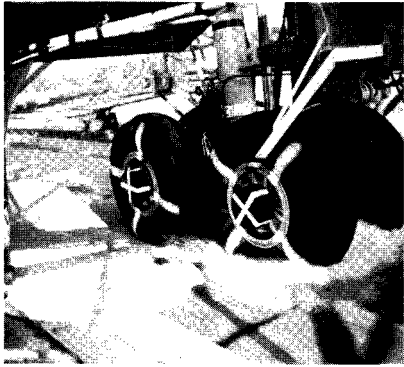
(a) Entrance into water;
V_G = 25 knots.
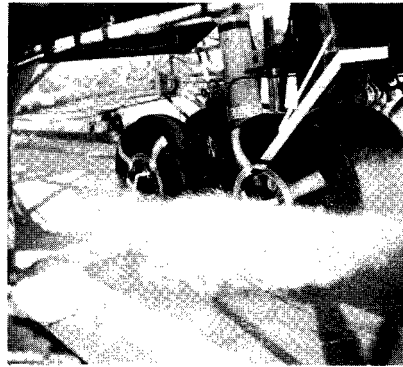
(b) $V_G/V_P \approx 0.32$;
V_G = 25 knots.
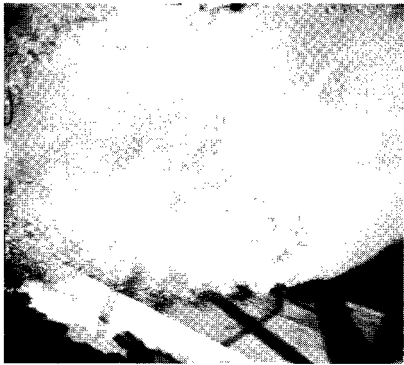
(c) $V_G/V_P \approx 0.32$;
V_G = 25 knots.

(d) $V_G/V_P \approx 0.64$;
V_G = 50 knots.
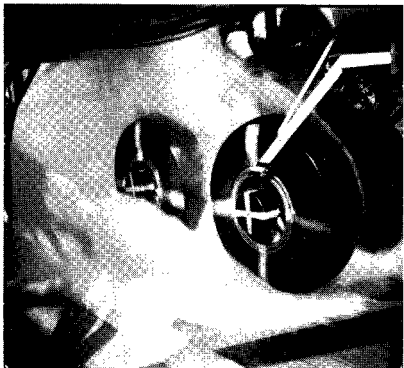
(e) $V_G/V_P \approx 0.96$;
V_G = 75 knots.
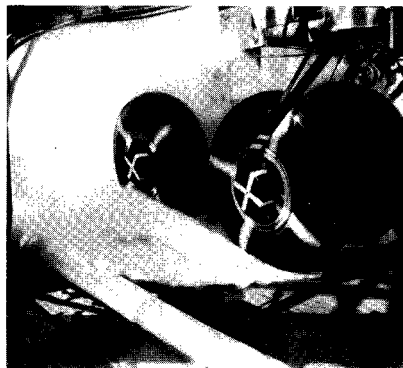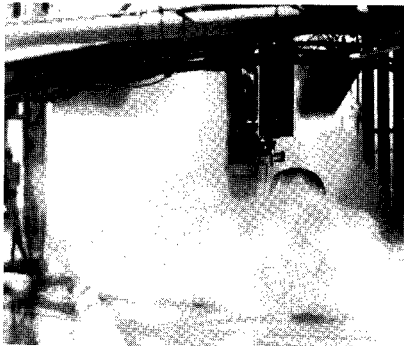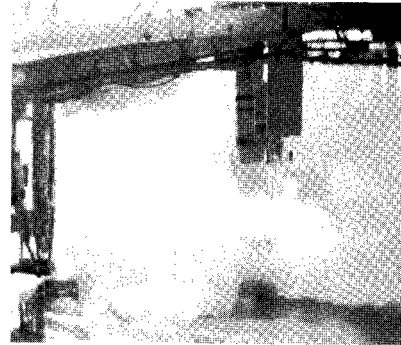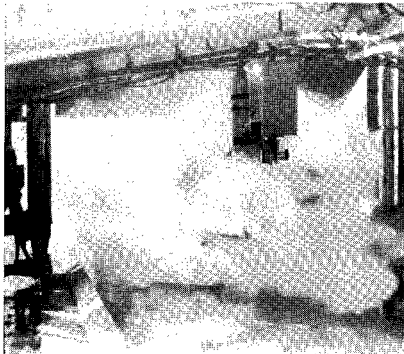

(f) $V_G/V_P \approx 1.23$;
V_G = 96 knots.

L-66-1185

Figure 23.- Spray patterns developed by dual tandem wheels (configuration I) at subhydroplaning and superhydroplaning velocities.
$F_{z,g} \approx$ 22 300 lb (99 195 N); p = 75 lb/in^2 (51.7 N/cm^2); 0.5 in.
(1.27 cm) water depth; oblique front view.
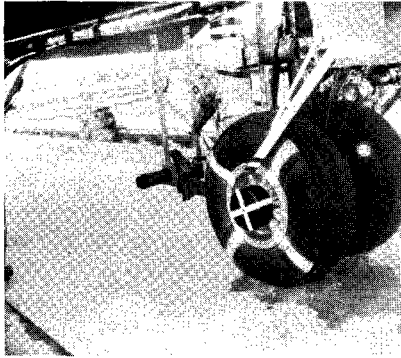
(a) Prior to entrance into water; V_G = 23 knots.
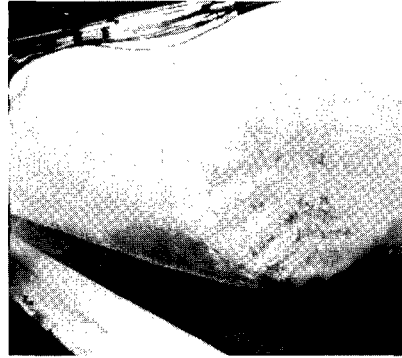

(b) $V_G/V_P \approx 0.29$; V_G = 23 knots; Water depth = 1.0 in. (2.54 cm).
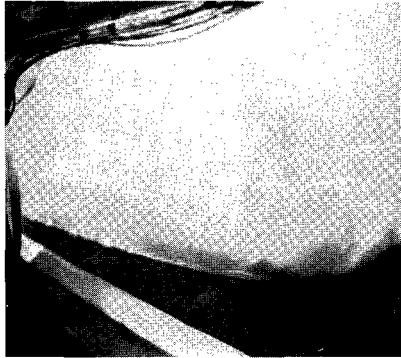
(c) $V_G/V_P \approx 0.72$; V_G = 56 knots; Water depth = 2.0 in. (5.08 cm).
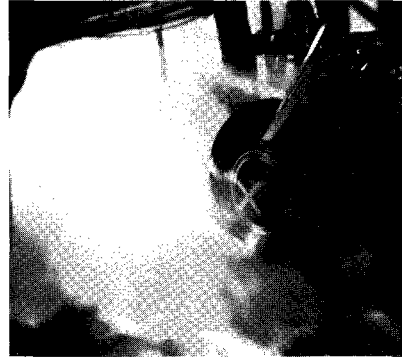
(d) $V_G/V_P \approx 1.01$; V_G = 79 knots; Water depth = 1.0 in. (2.54 cm).

(e) $V_G/V_P \approx 0.69$; V_G = 54 knots; Slush depth = 1.0 in. (2.54 cm).
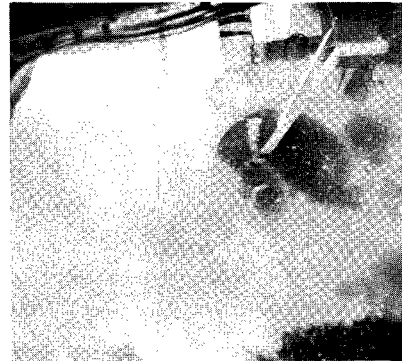
(f) $V_G/V_P \approx 1.01$; V_G = 79 knots; Slush depth = 1.0 in. (2.54 cm).

L-66-1186

Figure 24.- Spray patterns developed by dual front wheels (configuration II) at subhydroplaning and superhydroplaning velocities. $F_{z,g} \approx$ 12 000 lb (53 378 N); p = 75 lb/in^2 (51.7 N/cm^2); 1.0 and 2.0 in. (2.54 and 5.08 cm) water depth; 1.0 in. slush depth; oblique front view.
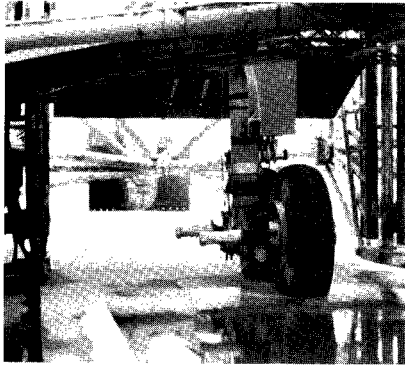
(a) Entrance into water;
V_G = 20 knots.
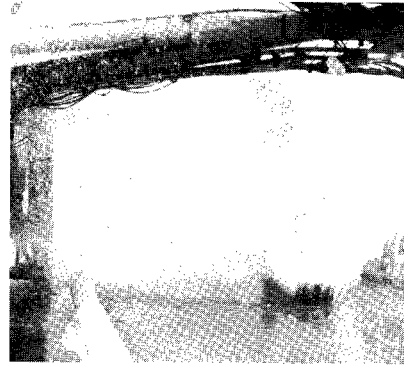
(b) $V_G/V_P \approx 0.44$;
V_G = 20 knots.
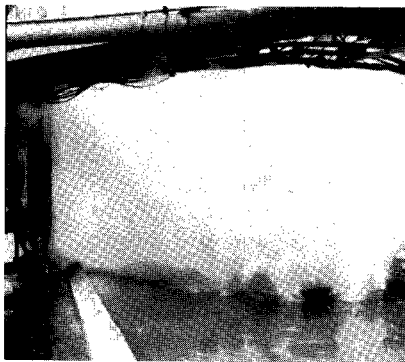
(c) $V_G/V_P \approx 0.93$;
V_G = 42 knots.
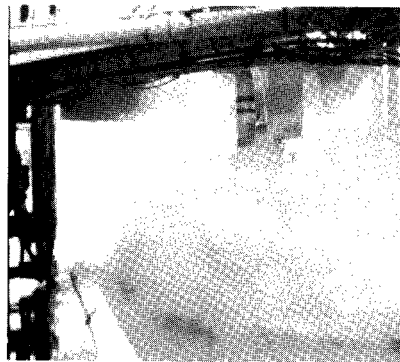
(d) $V_G/V_P \approx 1.29$;
V_G = 59 knots.
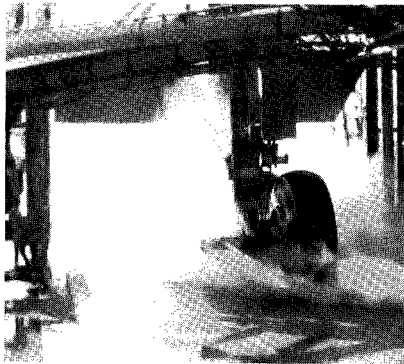
(e) $V_G/V_P \approx 1.71$;
V_G = 77 knots.
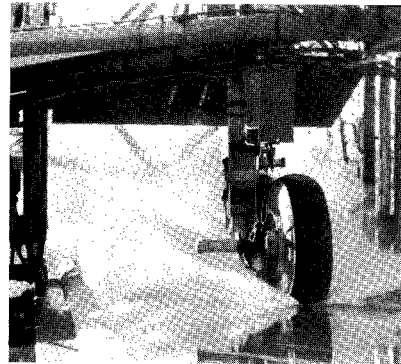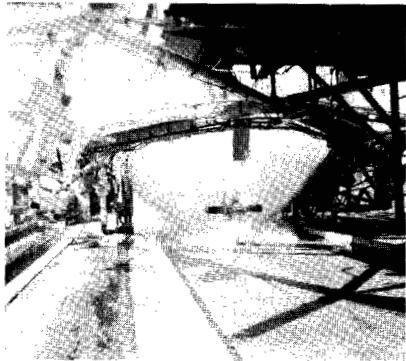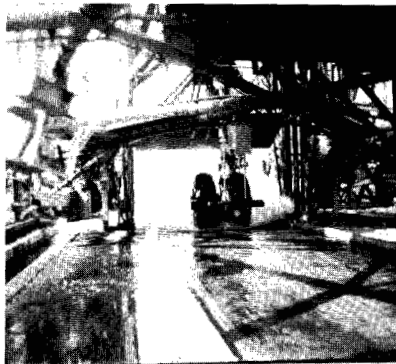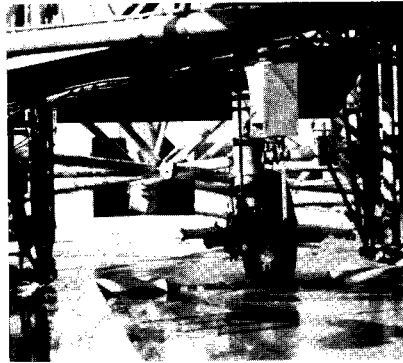
(f) $V_G/V_P \approx 2.22$;
V_G = 100 knots.

L-66-1187

Figure 25.- Spray patterns developed by single tandem wheels (configuration V) at subhydroplaning and superhydroplaning velocities.
$F_{z,g} \approx$ 12 000 lb (53 378 N); p = 25 lb/in^2 (17.2 N/cm^2); 1.0 in. (2.54 cm) water depth; oblique front view.

42
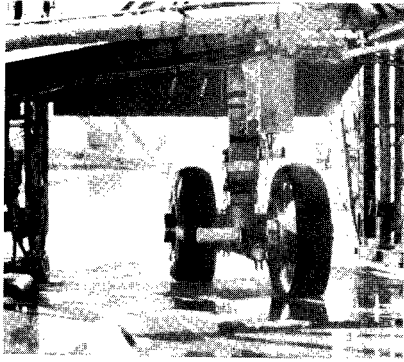
(a) Prior to entrance
into water;
$V_G = 24$ knots.
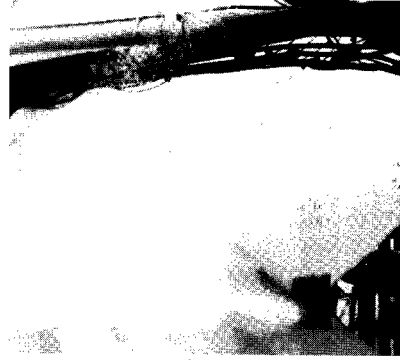
(b) $V_G/V_P \approx 0.53$;
$V_G = 24$ knots.

(c) $V_G/V_P \approx 1.20$;
$V_G = 54$ knots.

(d) $V_G/V_P \approx 1.29$;
$V_G = 59$ knots.

(e) $V_G/V_P \approx 1.71$;
$V_G = 77$ knots.
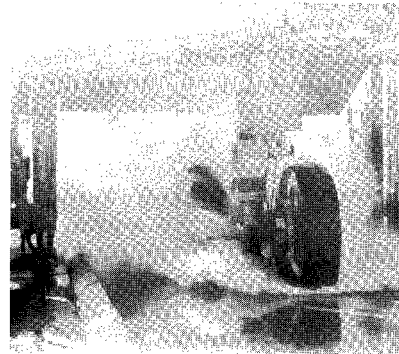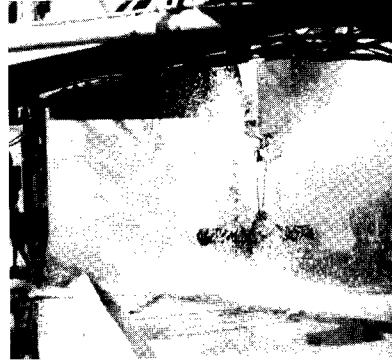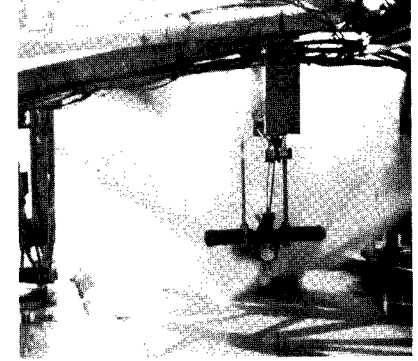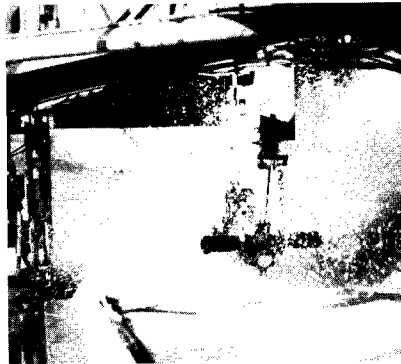

(f) $V_G/V_P \approx 2.22$;
$V_G = 100$ knots.

L-66-1188

Figure 26.- Spray patterns developed by diagonal wheels (configuration IV) at subhydroplaning and superhydroplaning velocities. $F_{z,g} \approx 12\ 000$ lb $(53\ 378$ N$)$; $p = 25$ lb/in^2 $(17.2$ N/cm$^2)$; 1.0 in. $(2.54$ cm$)$ water depth; oblique front view.
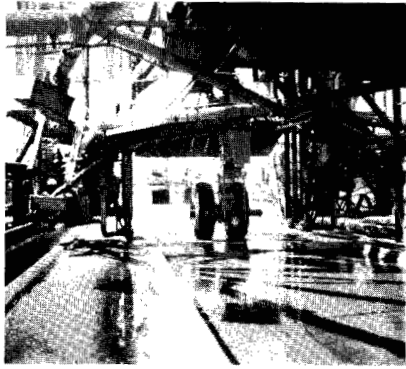
(a) Prior to entrance
into water;
V_G = 37 knots.
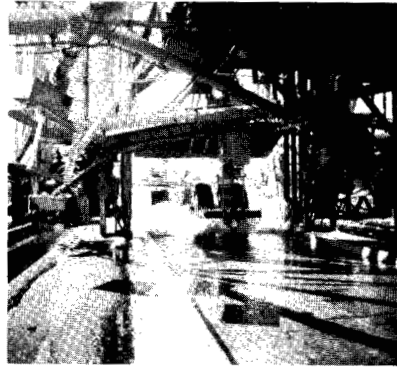
(b) Entrance into water;
$V_G/V_P \approx 0.47$;
V_G = 37 knots.

(c) $V_G/V_P \approx 0.55$;
V_G = 43 knots.

(d) $V_G/V_P \approx 0.87$;
V_G = 68 knots.
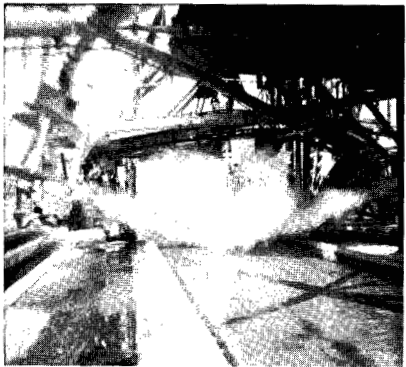
(e) $V_G/V_P \approx 1.00$;
V_G = 78 knots.

(f) $V_G/V_P \approx 1.23$;
V_G = 96 knots.

L-66-1189

Figure 27.- Spray patterns developed by dual rear wheels (configuration III) at subhydroplaning and superhydroplaning velocities.
$F_{z,g} \approx$ 12 000 lb (53 378 N); p = 75 lb/in^2 (51.7 N/cm^2); 1.0 in.
(2.54 cm) water depth; oblique front view.

Water depth = 1.0 in. (2.54 cm)

(a) Prior to entrance
into water;
V_G = 20 knots.

(b) $V_G/V_P \approx 0.25$;
V_G = 20 knots.

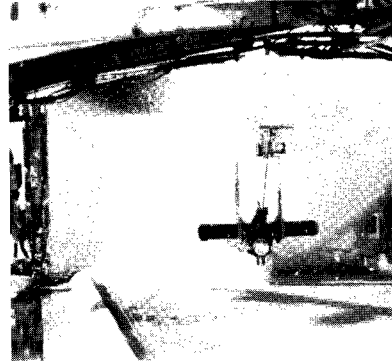(c) $V_G/V_P \approx 0.55$;
V_G = 43 knots.

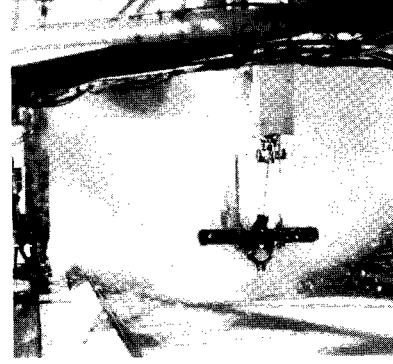(d) $V_G/V_P \approx 0.80$;
V_G = 63 knots.
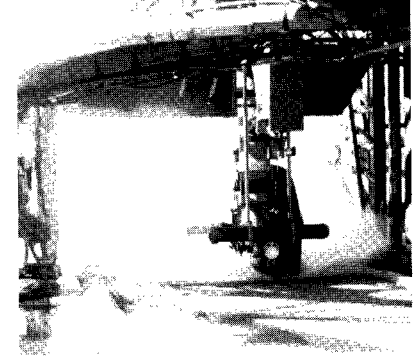
Slush depth = 1.0 in. (2.54 cm)

(e) $V_G/V_P \approx 0.35$;
V_G = 27 knots.

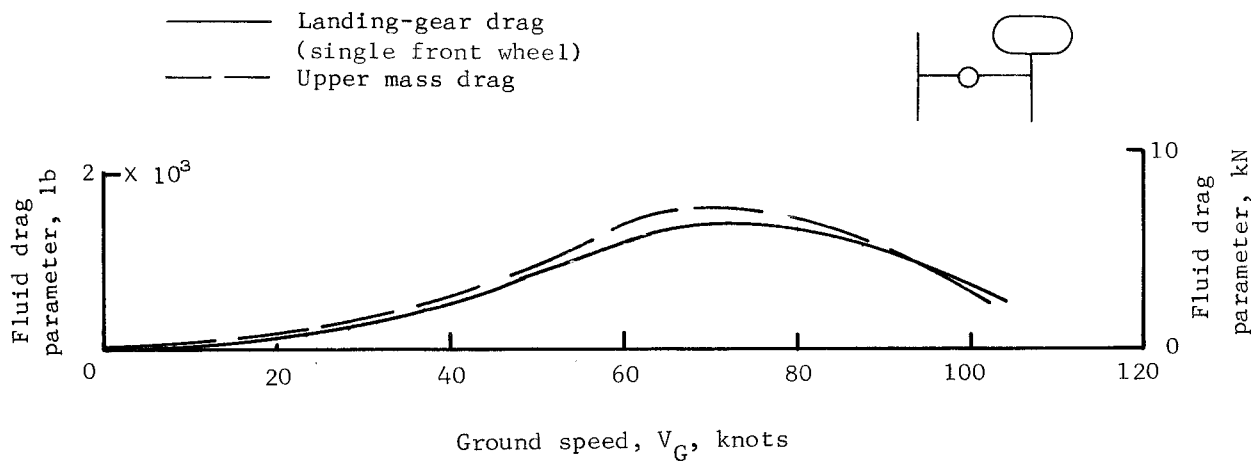(f) $V_G/V_P \approx 0.60$;
V_G = 47 knots.
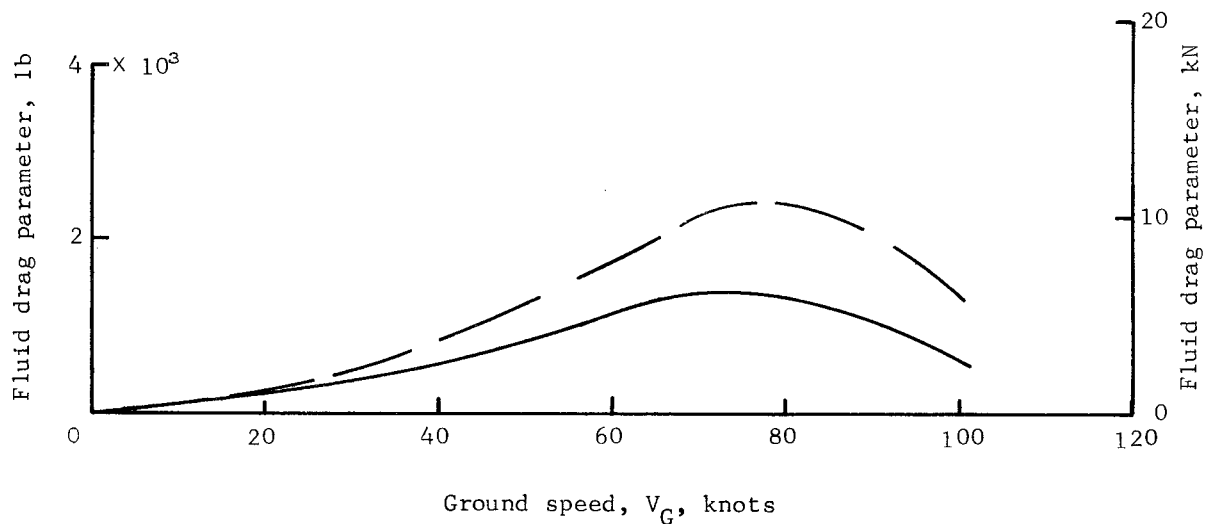
(g) $V_G/V_P \approx 0.91$;
V_G = 71 knots.

(h) $V_G/V_P \approx 1.33$;
V_G = 104 knots.

L-66-1190

Figure 28.- Spray patterns developed by single rear wheel (configuration VII) at subhydroplaning
and superhydroplaning velocities. $F_{z,g} \approx 12\ 000$ lb (53 378 N); p = 75 lb/in^2 (51.7 N/cm^2);
oblique front view.

45

(a) Flap angle = 22°.

(b) Flap angle = 55°.

Figure 29.- Comparison of drag parameter with ground speed for single
front wheel (configuration VI) with simulated wing flap at different
angles. $F_{z,g} \approx 12\ 000$ lb (53 378 N); p = 75 lb/in^2 (51.7 N/cm^2);
$d_1 \approx 1.0$ in. (2.54 cm).

46

Frame   1   6   10   12

             13   14   16   17

(a) Frames 1 to 17.   L-66-1191

Figure 30.- Pitching instability of bogie landing gear developed during test at light weight and high tire pressure (small vertical tire deflection) at superhydroplaning speed.

V_G = 100 knots; $F_{z,g} \approx$ 12 000 lb (53 378 N); $\frac{V_G}{V_P} \approx$ 1.29; p = 75 lb/in^2 (51.7 N/cm^2); 1.0 in.

(2.54 cm) water depth; bogie gear not equipped with pitch damper.

18   21   23   24

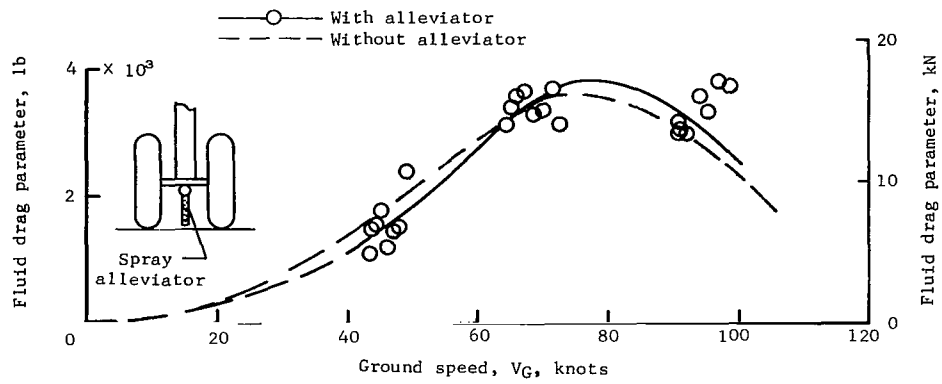27   29   30   32

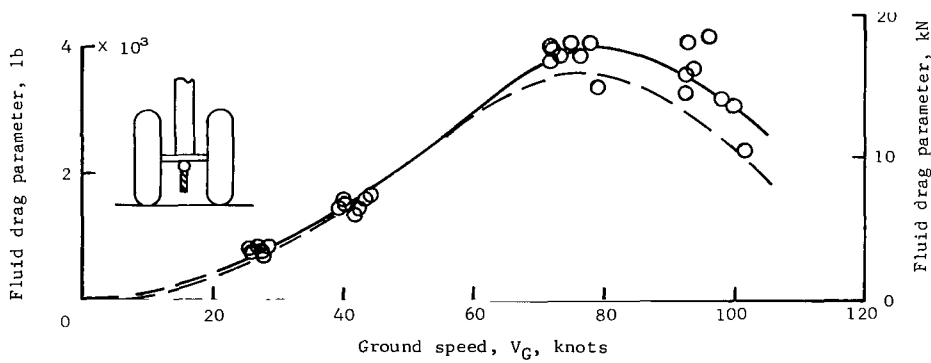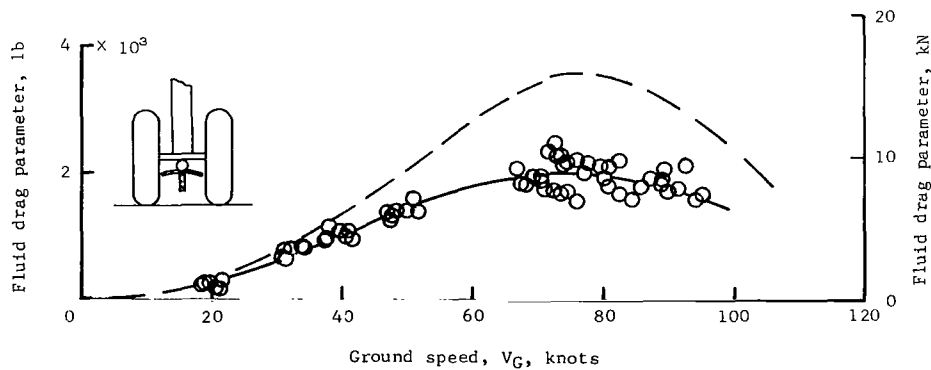(b) Frames 18 to 32.   L-66-1192

Figure 30.- Concluded.

(a) Flexible rubber alleviator.

(b) Rigid metal alleviator.

(c) Rigid metal alleviator with curved top.

Figure 31.- Variation of drag parameter with ground speed in water for dual tandem-wheels with and without spray-drag alleviators. $p = 75$ lb/in^2 (51.7 N/cm^2).

"The aeronautical and space activities of the United States shall be conducted so as to contribute . . . to the expansion of human knowledge of phenomena in the atmosphere and space. The Administration shall provide for the widest practicable and appropriate dissemination of information concerning its activities and the results thereof."

—NATIONAL AERONAUTICS AND SPACE ACT OF 1958

NASA SCIENTIFIC AND TECHNICAL PUBLICATIONS

TECHNICAL REPORTS: Scientific and technical information considered important, complete, and a lasting contribution to existing knowledge.

TECHNICAL NOTES: Information less broad in scope but nevertheless of importance as a contribution to existing knowledge.

TECHNICAL MEMORANDUMS: Information receiving limited distribution because of preliminary data, security classification, or other reasons.

CONTRACTOR REPORTS: Technical information generated in connection with a NASA contract or grant and released under NASA auspices.

TECHNICAL TRANSLATIONS: Information published in a foreign language considered to merit NASA distribution in English.

TECHNICAL REPRINTS: Information derived from NASA activities and initially published in the form of journal articles.

SPECIAL PUBLICATIONS: Information derived from or of value to NASA activities but not necessarily reporting the results of individual NASA-programmed scientific efforts. Publications include conference proceedings, monographs, data compilations, handbooks, sourcebooks, and special bibliographies.

Details on the availability of these publications may be obtained from:

SCIENTIFIC AND TECHNICAL INFORMATION DIVISION

NATIONAL AERONAUTICS AND SPACE ADMINISTRATION

Washington, D.C. 20546